Developing Methodology to Prepare a Nanoparticle Coated Crystal for Infrared Analyses in Order to Specifically Identify Changes to Molecules that Coat the Surface

Submitted to:

The Engineering Honors Committee
244 Hitchcock Hall
College of Engineering
The Ohio State University

By:

Craig Ayres
Environmental Engineering Undergraduate
39 W 10th Ave Apt B
Columbus, OH 43201

Under the supervision of:

Dr. John Lenhart
Professor of Civil and Environmental Engineering
The Ohio State University
417A Hitchcock Hall
2070 Neil Avenue
Columbus, OH 43210

April 5th, 2013

Abstract

The widespread use of nanomaterials demonstrates a tremendous benefit to society; however, as nanomaterials are inevitably introduced to the environment, it is unknown how their compositions and coating agents alter in different settings and over a prolonged period of time. Coating agents are applied either during or post synthesis to prevent aggregation. Tracking changes to the molecules that coat the surface of nanomaterials is imperative to understanding the inherent risk when nanomaterials are released to the environment. The purpose of my research is to develop a method to prepare a nanoparticle coated crystal for infrared (IR) analyses in order to specifically identify changes to molecules that coat the surface.

The two nanomaterials analyzed in this study were hematite and nanosilver. Citrate was the primary coating agent used on both materials. The particles were coated to IR crystals and the coating layers were evaluated under static and dynamic conditions. Variables included coating agent (water, citrate, phthalic acid) and pH. Previously collected data from batch adsorption experiments of citrate and phthalic acid on hematite were used to validate the static system method for hematite. The static experiments successfully detected the adsorption of citrate on the surface of both hematite and nanosilver. The largest issue involved resolving the spectra; specifically, removing the IR absorption of water. This presence of water proved to be an even greater obstacle in the flow-through cell; however, the most successful method involved subtracting water spectra from each component before resolving. No spectra were obtained from silver perhaps due to the silver not adhering to the flow-through cell surface.

Significant progress has been made and once the influence of water is removed, these processes should have a vast potential for further research to determine specific changes to nanoparticle surfaces, particularly with the flow-through cell for greater control over variability.

Acknowledgements

This research project would not have been possible without the support and guidance of Dr. John Lenhart and Matt Noerpel. I would like to thank Dr. Lenhart for advising me through the research process and my entire senior year as well as fueling my interest to expand upon the knowledge obtained in the classroom. I am very grateful to Matt Noerpel for not only teaching me everything in the lab from infrared spectroscopy to cleaning up hematite spills but also answering each of my seemingly infinite questions. The support from both of them was integral to the success of this research.

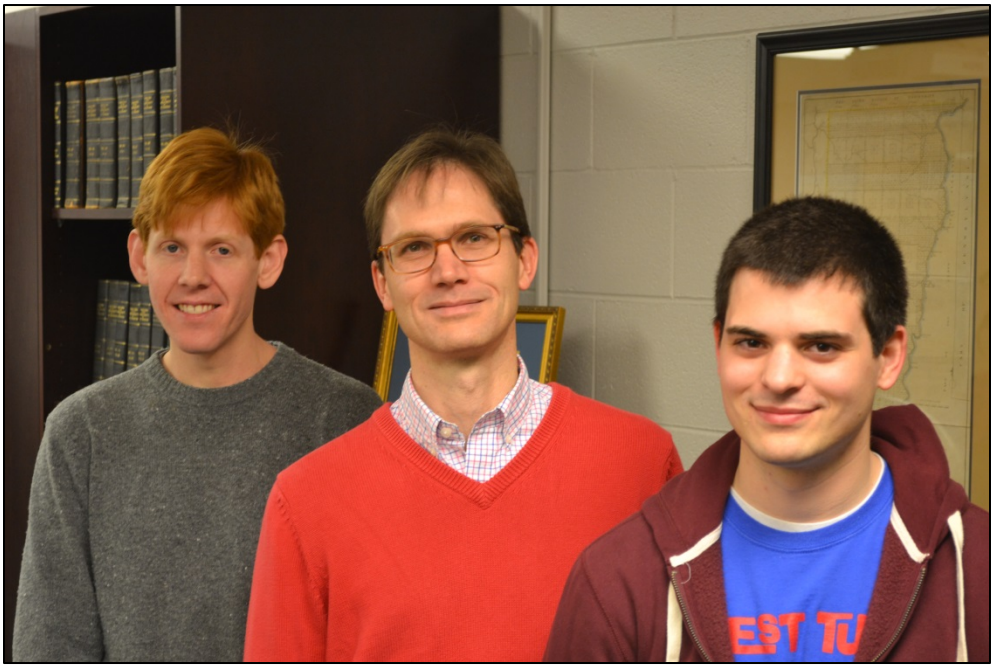

Table of Contents

Chapter 1:

Introduction

1.1 Nanoparticle Background

Nanoscience and nanotechnology involve the synthesis, assembly, manipulation, and application of materials on the nanometer-scale level that spans approximately 1 to 100 nm at two- or three-dimensions [1]. Nanotechnology itself refers to the integration of these nanoscale structures into larger material components and systems, keeping the control and construction of new and improved materials at the nanoscale [2]. The small stature of nanoparticles results in a large surface area to volume ratio. This is an extremely significant property of nanoparticles as it allows for a greater number of surface atoms and therefore considerable surface energy and reactivity. The high surface energy indicates that particles on the nanoscale may exhibit enhanced properties relative to the bulk material and that the magnitude of these properties increases with a decrease in size. While nanoparticles exist naturally in the environment, manufactured nanoparticles have become appealing for industrial purposes because they can be produced and manipulated with relative ease. Manufactured nanoparticles are utilized more than any other nanomaterial in a variety of areas including pharmaceuticals, cosmetics, electronics, optical devices, environmental remediation, catalysis chemistry and material sciences [3-5]. Nanoparticles are generally divided into two classifications: organic and inorganic. Examples of organic nanoparticles are fullerenes (C_{60}) and carbon nanotubes. Materials containing carbon nanotubes may be strong enough to build spacecrafts, conduct twice the electricity of copper, and improve rechargeable batteries and fuel cell production [6]. Inorganic nanoparticles include metals, metal oxides, and quantum dots. Silver nanoparticles, or nanosilver, has substantial antibacterial properties and is thus widely commercialized for consumer products and medical

purposes. Nanosilver may be used in various clothing items such as socks, to restrict the growth of odor-causing bacteria [7]. Figure 1 is an image of sock material containing spherical silver particles from Benn et al. [7]

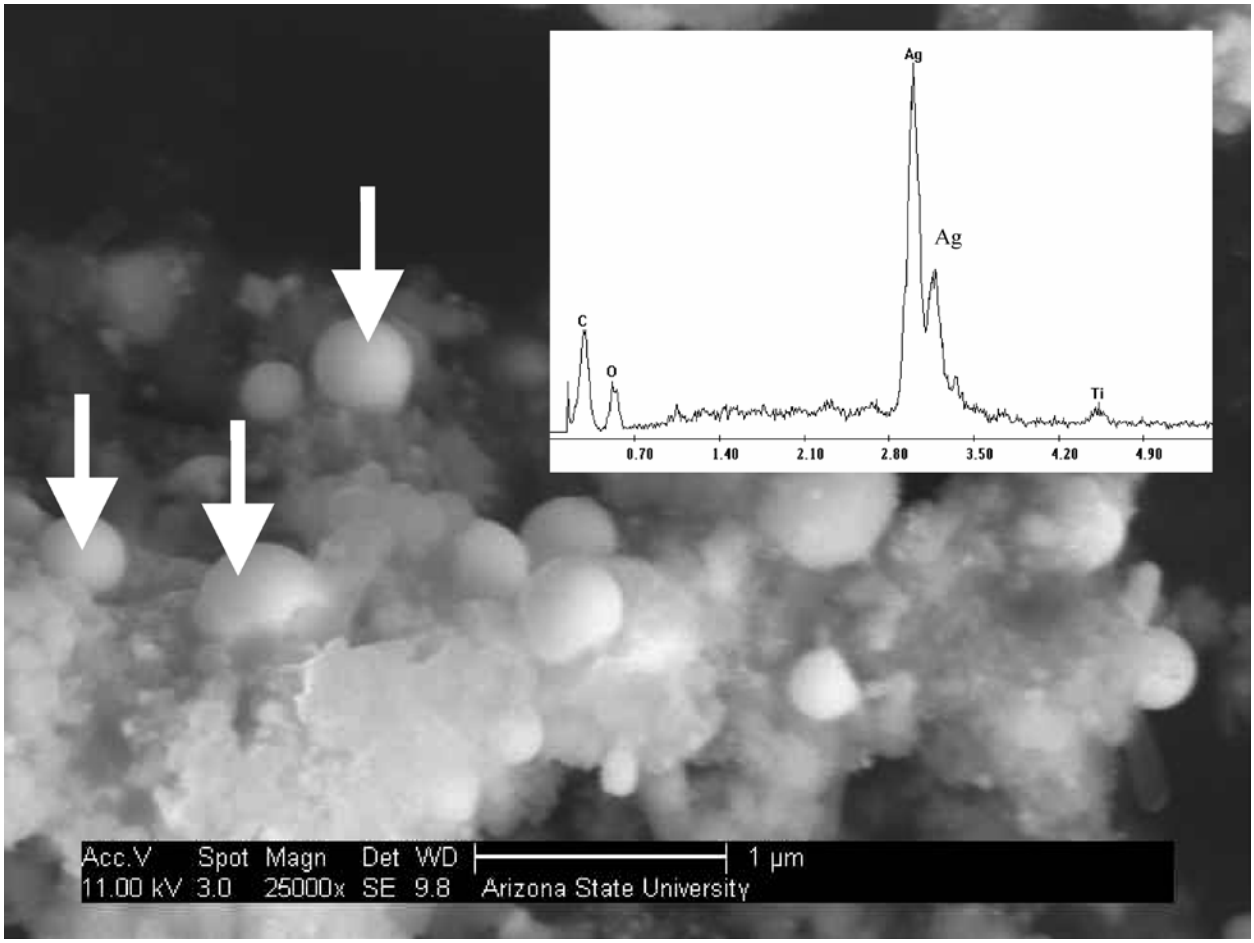

Figure 1: SEM image of sock material showing spherical silver particles on the order of 100 nm in diameter. Inset: Representative EDX analysis of the spherical silver particles marked with white arrows [7]

Quantum dots are small assemblies of semiconductor materials in the range of 2-10 nm, and they possess unique electronic, optical, magnetic, and catalytic properties [8]. While holding great potential for application in such fields as molecular biology, quantum dots are generally comprised of extremely toxic materials i.e. cadmium, sulfur, selenium, and tellurium.

Nanomaterials may enter and accumulate in air, water, soil, or organisms from point sources such as factories or landfills, as well as from nonpoint sources, such as wet deposition from the atmosphere, storm-water runoff, and attrition from nanomaterial-containing products [9,10]. Among the likely routes of discharge of nanomaterials into the environment, the release of commercial nanoparticles into natural waters through the discharge of treated municipal sewage attracts the most concern [7]. After entering a water body, the fate of these nanomaterials depends upon transport (aggregation, deposition, adsorption, bioaccumulation) and transformation (oxidation, reduction, dissolution, bio- and UV-degradation) processes [11]. The impact of these processes on determining nanomaterial fate is currently poorly understood. In addition, the risk posed by such materials to human health and the environment is unclear, although preliminary evidence exists to suggest certain nanomaterials may harm people, organisms or the environment [12]. Research has shown that exposure to nanomaterials may produce effects that differ from those observed with conventionally scaled materials. Some nanomaterials may cross the human blood-brain or placental barrier in ways that larger particles cannot [13]. The exposure routes of nanoparticles are described in Table 1.

Table 1: Consumer exposure for several types of nanomaterial products [13]

Product type	Release and/or exposure source	Exposed population	Potential exposure route
Sunscreen	Product application by consumer to skin	Consumer	Dermal
	Release by consumer to water supply (e.g., washing with soap and water)	General population	Ingestion
	Disposal of sunscreen container with residual sunscreen after use to landfill or incineration	General population	Inhalation or ingestion
Paints and coating	Weathering, disposal	Consumers, general population	Dermal, inhalation or ingestion
Clothing	Wear, washing, disposal	Consumers, general population	Dermal, inhalation, ingestion from surface or ground water
Electronics	Release at end of life or recycling stage	Consumers, general population	Dermal, ingestion from surface or ground water
Sporting goods	Release at end of life or recycling stage	Consumers, general population	Dermal, inhalation, ingestion from surface or ground water

1.2 Surface Coating Overview

The high surface area to volume ratio of the nanoparticles results in high reactivity which leads to particle aggregation and settling, negating the desired properties. To prevent particle aggregation a coating or capping agent is applied either during or post synthesis. Surface coatings can be organic molecules, polymers, or biological molecules. Coatings generally work by either charge or steric stabilization mechanisms, which prevent further aggregation [14]. Citrate is a common capping agent for stability but is also used in analysis to model polycarboxylic acids ubiquitously found in nature. In addition to stabilization, coatings can be carriers of specific functionalities for further applications [14]. Coatings can also affect bactericidal properties. For example, several studies have observed toxic effects from positively charged nanoparticles, but these effects are not seen when the same particles are coated with negatively charged functional groups. Understanding the effects of surface chemistry on the fate

of nanoparticles in the environment is imperative to designing coatings that maximize their effectiveness while minimizing any negative ecological consequences [10].

1.3 Objectives

The purposes for this study were to (1) develop a method to prepare a particle coated IR surface, (2) couple this to a flow-through cell for dynamic changes, and (3) implement the method for analysis. Tracking changes to the molecules that coat the surface of nanomaterials is imperative to understanding the inherent risk when nanomaterials are released to the environment. Factors analyzed in the dynamic, flow-through system include pH and coating agent. This proposal is part of a larger project within the research group of Dr. John Lenhart of The Ohio State University to further understand the fate of nanomaterials as they migrate through soils. The methodology developed in this study shall theoretically be applicable to various nanomaterials and coating agents.

Chapter 2:

Materials and Methods

2.1 Overview

The research consisted of several steps involving synthesis, characterization, and infrared analyses. The main constraint in the process is utilizing the hardware that is already in house. Also, while nanosilver is the preferred subject of analysis, hematite (α-Fe_2O_3) was studied first because it is more stable and easily synthesized. Also, there is a great deal of familiarity with hematite and its infrared spectra from previous studies in the lab that allow for convenient comparison. The majority of necessary equipment for this research is located in the environmental engineering research laboratory in Hitchcock Hall although other instruments such as the TEM were utilized on other areas of campus.

The initial step is synthesis of the nanomaterials. There are various procedures for the synthesis of nanosilver or nano-sized iron oxide particles. In general, they begin with a salt of the respective metal (i.e. ferric chloride for the iron oxide particles) that is added to a solution to achieve a desired metal concentration. Hematite particles were prepared based on the procedure described by Matijevic and Scheiner [15]. The procedure produces roughly spherical particles around 50 nm in diameter. Silver nanoparticles were synthesized by the reduction of the $[Ag(NH_3)_2]^+$ complex with D-maltose following the method described by Kvítek et al. [16]. The procedure produces spherical particles around 50 nm in diameter. The main parameters controlling the particle size are reducing sugar and ammonia concentration. Nanosilver synthesis is sensitive to light and reaction time, so caution was taken in these regards.

Once synthesized, the next step is to characterize the nanoparticles to ensure proper composition and size has been achieved. The nanoparticle solutions were initially placed in a Zeta Plus Particle Size Analyzer (Brookhaven Istr. Co.) to determine the average hydraulic

radius. Further determination of size and morphology was obtained using transmission electron microscopy (TEM). Surface area of the hematite was analyzed using the BET method.

Attenuated total reflection infrared (ATR-FTIR) spectroscopy has been widely used to study adsorption of organic ligands on mineral interfaces as it is a surface sensitive technique capable of providing information on the individual processes at the mineral-water interface [17]. Initially, this procedure was implemented in a static manner for convenience purposes. In this case, a thin layer of the nanoparticle solution is applied to the ATR crystal surface and gently dried. Upon coating the crystal, a small volume of a desired coating agent or acid may be placed on top of the crystal in order to analyze the interactions on the surface of the nanoparticle. Once sufficient experience with the static system was obtained, a flow-through cell was utilized where particles would adsorb to the nanoparticle surface in a continuous manner. This approach enables for a dynamic system that increases the control over variability in such factors as pH and ionic strength. The results of the ATR-FTIR spectroscopy entail a plot of absorbance versus wavelength. Various spikes in the plot relate to vibrational frequencies of respective chemical moieties that contain dipole moments. This data allows for the possible determination of the chemical composition and structure of the coating agents.

Citrate was the primary capping agent studied as it can be applied to synthesis procedures as well as fate assessment, modeling ubiquitous organic acids found in nature. There was also a great deal of experience and data for comparison regarding citrate adsorption to hematite. The term “Citrate” is used in this paper to convey the gamut of species from citric acid (fully protonated) to citrate ion (fully deprotonated) as analyses occur over a wide range of pH values. Figure 2 depicts the distribution of these various citrate species as a function of pH.

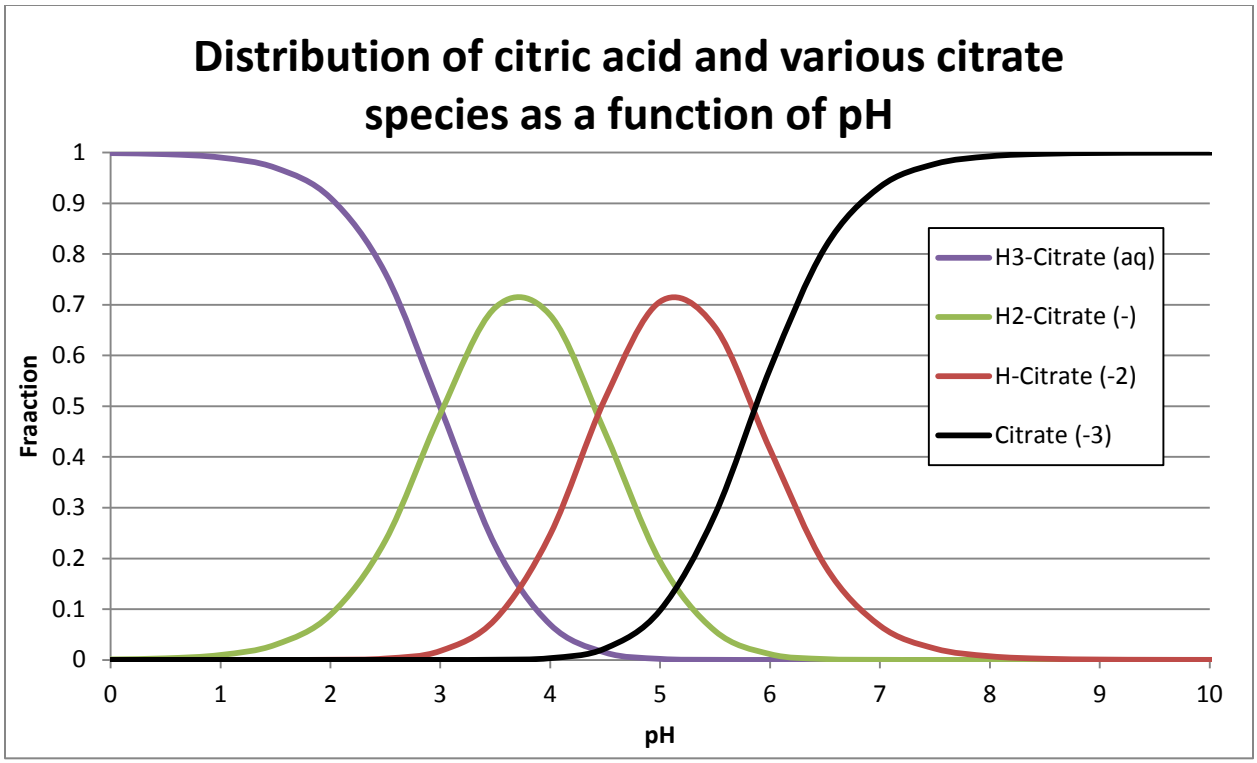

Figure 2: Citrate species as a function of pH. H, H2, and H3 correspond to the hydrogens present. Citric acid is fully protonated while citrate (-3) is fully deprotonated. Number in parentheses represents the charge.

According to Figure 2, citric acid begins to lose its first hydrogen proton around a pH of 3. This is also evident in Figure 3, the IR spectra for citrate in the liquid phase as a carbonyl group (1720 cm^{-1}) is present at pH=3.47 however increasing the pH to 5.55 removes that peak. This is due to citric acid becoming H_2-Citrate as a hydrogen ion is removed from the carbonyl group. The asymmetric stretch (1570 cm^{-1}) corresponds to a wagging motion where the species move in and out in opposite directions. The symmetric stretch (1390 cm^{-1}) corresponds to a rocking motion where the species simultaneously move in and out in the same manner. These stretches are inversely related to the functional groups, i.e. losing a hydroxyl group enables greater motion and an increase in the asymmetric peak. The liquid phase spectra are important when determining how the molecules adsorb to the surface. A significant change in between the liquid phase spectra and adsorbed spectra indicates a change in molecular structure.

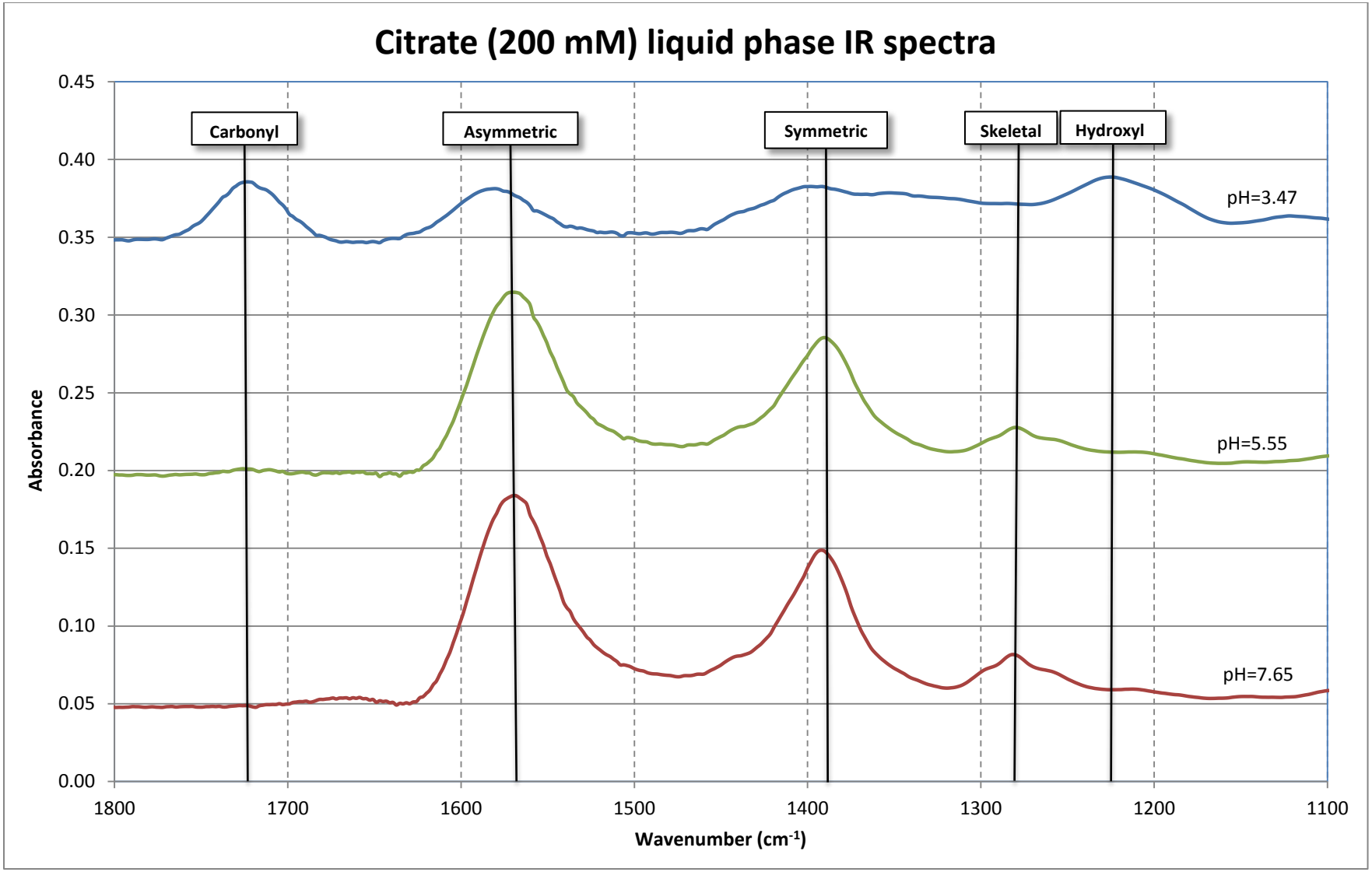

Figure 3: IR spectra for citrate (200 mM) solution at various pH values. Boxes indicate the action correlating to each peak. Data obtained from Noerpel et al [19]

2.2 Synthesis of Hematite

Before beginning the hematite synthesis, it was necessary to ensure all glassware was properly cleaned. Approximately 10-20 mL of concentrated HCl was added to the 2 L bottle and it remained closed overnight. The other glassware was soaked in a 10% nitric acid wash overnight, rinsed with deionized water, and oven-dried under dust-free conditions. 10.812 g $FeCl_3$-$6H_2O$ were crushed and placed in a 50 mL volumetric flask. This hexahydrate compound was chosen over the anhydrous form because the anhydrous form would collect water from the atmosphere at too rapid of a pace to make an accurate determination of weight or concentration. The flask was then filled to 50 mL with 0.004 M HCl solution. The ferric chloride solution remained overnight to ensure complete dissolution. The 50 mL ferric chloride solution was then filtered into a beaker through a (0.22 µm) PVDF syringe filter and added to 1950 mL of 0.004 M HCl solution that had been preheated to 98°C. The suspension was aged in a closed 2 L vessel at 98°C for 3 days, after which it was rapidly cooled to room temperature. Solid NaOH was then added which allowed for flocculation and sedimentation of the iron particles, isolating them from the solution. The supernatant was decanted to less than 50 mL of concentrated solution. The concentrate was then transferred to 8000-10000 Dalton dialysis tubing and dialyzed against deionized water to remove excess salts and amorphous solids. The dialysis water was changed twice per day for 4-6 days followed by dialysis against 0.001 M $HClO_4$ for one day. This suspension was stored in an amber glass bottle at 4°C.

2.3 Synthesis of Silver Nanoparticles

Colloidal silver nanoparticles are produced by the reduction of $[Ag(NH_3)_2]^+$ complex known as the “silver mirror” reaction or Tollens process [16]. Because silver is photosensitive,

all solutions containing silver were either wrapped in foil or placed under a box. The following solutions were used for synthesis of the silver nanoparticles as stated in Panacek et al. (2006): 0.01 M silver nitrate, 0.02 M ammonia, 0.10 M NaOH, and 0.025 M D-maltose ($C_{12}H_{22}O_{11}$) [18]. All four reagents were removed from the fridge for at least 2 hours before synthesis to equilibrate the solutions to room temperature. Each reagent was also filtered through a (0.2 µm) PVDF syringe filter into individual beakers. Desired volumes were then pipetted from the beakers. First, 2 mL of the silver nitrate solution was pipetted into a 50 mL glass beaker followed by 10 mL of the ammonia solution. A small, magnetic stir bar mixed the solution at a slow speed. The pH of the solution was then adjusted to 11.5 upon addition of 250 µL of sodium hydroxide. Lastly, 8 mL of D-maltose was added to reduce the silver ammonia complexes. This reaction lasted approximately 15 minutes in a light-prohibited environment. If synthesis has occurred the solution will appear bright orange.

Immediately following the synthesis, the nanosilver suspension was dialyzed against deionized water to remove residual ions and D-maltose. 8000-10000 Dalton dialysis tubing was used and clamped shut at both ends. The dialysis occurred over several days with four complete changes of the deionized water. Throughout dialysis, a box was placed on top of the solution to prevent light penetration.

2.4 Characterization of Nanoparticles

Ideal experimental conditions include a fixed size distribution and morphology. A Zeta Plus Particle Size Analyzer (Brookhaven Istr. Co.) and transmission electron microscopy (TEM) were used to determine the size and morphology of the synthesized samples. A BET surface area test was also applied to the hematite samples. As previously mentioned, the hematite

nanoparticles exhibit a roughly spherical shape. The BET surface area test is therefore executed to determine the extent of its spherical nature by comparing the surface area to its determined diameter. This test also allows for the determination of available adsorption sites.

2.5 Infrared Analysis

Attenuated total reflectance-Fourier transform infrared (ATR-FTIR) spectroscopy was utilized for its ability to detect processes occurring on the surface of the mineral. ATR-FTIR techniques release infrared waves that will be absorbed and excite bonds at their characteristic wavelengths. The type of molecular bond may be determined from the wavenumber of an absorption peak and its respective amplitude and shape. ATR-FTIR spectra were collected with a Nicolet Nexus 670 Infrared Spectrometer. A nine-bounce diamond cell (DurasamplIR) was used in the static system experiments while a 20 bounce, 2 mm thick germanium cell was used in the dynamic, flow-through system experiments. The germanium cell has a penetration depth of 0.65 μm. The penetration depth is significant because it should be greater than or equal to the coating on the cell in order to detect interactions at the surface of the particles. Consequently, the solution must be diluted to undetectable levels to isolate the interactions at the surface. Data collection and spectral analyses including subtraction were performed using OMNIC (version 6.1a, Thermo Nicolet Corporation).

2.5.1 Static System

The static system experiments involved coating the infrared crystal with a respective nanomaterial and then placing a small volume of supernatant – i.e. a coating agent or acid – on top of the coated crystal. ATR-FTIR measurements were performed on hematite coatings, silver coatings, aqueous citric acid solution, and aqueous phthalic acid solution. The hematite coating

was applied by creating a solution of equal parts hematite and bio-grade ethanol. A thin layer of the resulting solution was applied to the diamond crystal and spread evenly with a stream of nitrogen. To ensure the hematite was entirely dried and to remove excess material, the crystal was rinsed with deionized water and once again dried with nitrogen. The initial attempt at coating the crystal with silver involved placing a small volume of solution on the crystal and evenly distributing with nitrogen. The silver did not dry readily but after allowing the solution to dry overnight, spectra could be collected. Silver was also coated following the addition of equal parts of bio-grade ethanol and this solution would dry within a few minutes as nitrogen was applied.

Once the spectrometer is sufficiently warmed up, the first reading taken was the background. All ensuing readings were taken relative to this background spectrum. The next spectra collected are an empty cell followed by a coated cell. These may be used to subtract from subsequent spectra to reduce the effect of experimental noise and generate a smoother curve. The supernatant solutions were diluted to undetectable levels in order to isolate the interactions on the surface and ignore molecules in solution. Consequently, a water spectrum was necessary to subtract from the readings. The citric acid was diluted to 1 mM and the phthalic acid was diluted to 0.1 mM. When dealing with a supernatant over the coated crystal, the sample holding region was covered with a lid to prevent evaporation and interactions with air molecules from occurring. Previously collected spectra of hematite wet paste at various pH values were also occasionally subtracted from the results in order to remove the effect of the hematite itself.

2.5.2 Dynamic Flow-through System

The dynamic flow-through system was implemented for increased control over variability. This system (depicted in Figures 4 and 5) consisted of a Mettler Toledo DL77X auto-titrator, Nicolet Nexus 670 Infrared Spectrometer, and HPLC pump. A pH electrode, stirrer, tube to inject titrant, and HPLC tubing were placed inside the titration vessel. Certain tests introduced a stream of nitrogen into the titration vessels to remove the presence of carbonate groups. The fluid inside the titration vessel was pumped to one end of the flow-through cell. Once the trough was flooded, the fluid was then pulled through to the pump and recycled back to the titration vessel. A flow rate of 3 mL/min was chosen as an adequate rate to ensure equilibrium was met without disturbing the crystal coating. Both the auto-titrator and spectrometer were controlled in an auxiliary fashion by computer programs. The titrator and spectrometer were controlled and monitored by LabX (version 1.20, Mettler Toledo) and OMNIC (version 6.1a, Thermo Nicolet Corporation) respectively. Methods were written into LabX to go through a progression of pHs, with adequate stir time in between titrations to allow for equilibrium to be reached and spectra to be collected. A macro was written in AutoIT (SciTE-Lite version 2.28) to execute the experiment by automation.

Figure 4: Image of flow-through system. The system includes an auto-titrator (1), infrared spectrometer (2), and a pump to transfer liquid from the auto-titrator to the spectrometer (3)

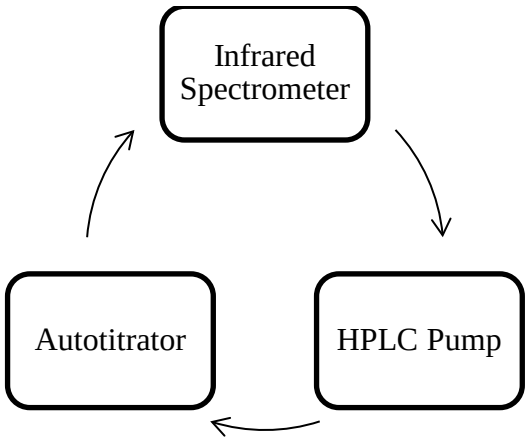

Figure 5: Illustration depicting mechanisms of flow-through cell. Fluid is pumped from the auto-titrator to one end of the infrared spectrometer flow-through cell. The fluid is then pulled through the other end and transferred back to the HPLC pump. From there the fluid is recycled back to the auto-titrator

Prior to analysis, the pump and flow-through cell were flushed with water to cleanse the tubing of any excess material. Next, the flow-through cell is removed and coated with the desired nanomaterial. The coatings were performed in similar fashion as the static system; however, the flow-through cell is much larger than the diamond cell and proved more difficult to coat evenly over such a great area. In order to decrease the viscosity and increase the volatility of the hematite supernatant, the solution was mixed with ethanol. 100 µL were used to coat the crystal surface and this solution was comprised of 75 µL of bio-grade ethanol and 25 µL of hematite solution for an ethanol to hematite ratio of 3:1. The nanosilver solution required much less ethanol with a maximum ratio of 1:1. Once coated and dried under nitrogen, the cell was rinsed with deionized water in order to remove excess particles and break up larger aggregates. Once a sufficient coating was achieved, the crystal was dried under nitrogen for approximately ten minutes to remove any trace of deionized water that may still be in the cell.

Similar to the static system, the first spectra collected were the background and empty cell. Both spectra were collected based on a dry coated cell. Next, a solution of deionized water and 100 mM NaCl was passed through the flow cell and spectra were collected at various pH values. The small amount of NaCl was added to the solution to increase the adsorption of the hematite. Initially, the pH is lowered to 3 and subsequently raised after each spectra collection using 0.1 M NaOH as the titrant. 10 minutes were allotted between the end of titration and beginning of the spectra collection to reach equilibrium at the adjusted pH. These hematite coated cells at various pH spectra were collected in order to subtract from the citrate samples, thus eradicating the effect of the hematite itself and water from the diluted citrate solution. Once a pH of 8.5 was achieved, the water solution was replaced with a solution of 1 mM citric acid and 100 mM NaCl set to an initial pH of 8.5. This citric acid solution was sequentially lowered

to a pH of 3.5 after each spectra collection using 0.1 HCl as the titrant. This method of titrating up with NaOH followed by titrating down with HCl was chosen to avoid a significant pH alteration at the transition. Once all readings have been taken, deionized water is run through the system while the flow-through cell is removed in order to clean the crystal of its hematite coating.

Chapter 3:

Results and Discussion

3.1 Synthesis and Characterization

The procedure followed for synthesis of hematite was designed to produce roughly spherical particles of 50 nm in diameter. Upon aging in a closed 2 L vessel at 98°C for 3 days, samples were taken, sonicated to remove aggregates, and placed in the Zeta Plus Particle Size Analyzer (Brookhaven Instr. Co.) for initial determination of effective diameter. The results obtained from the Particle Size Analyzer were taken before dialysis and thus served as preliminary measurements to ensure the synthesis had occurred properly. Final determinations of size and morphology were subject to analysis through TEM. Several images were captured from the TEM analysis such as Figure 6 below:

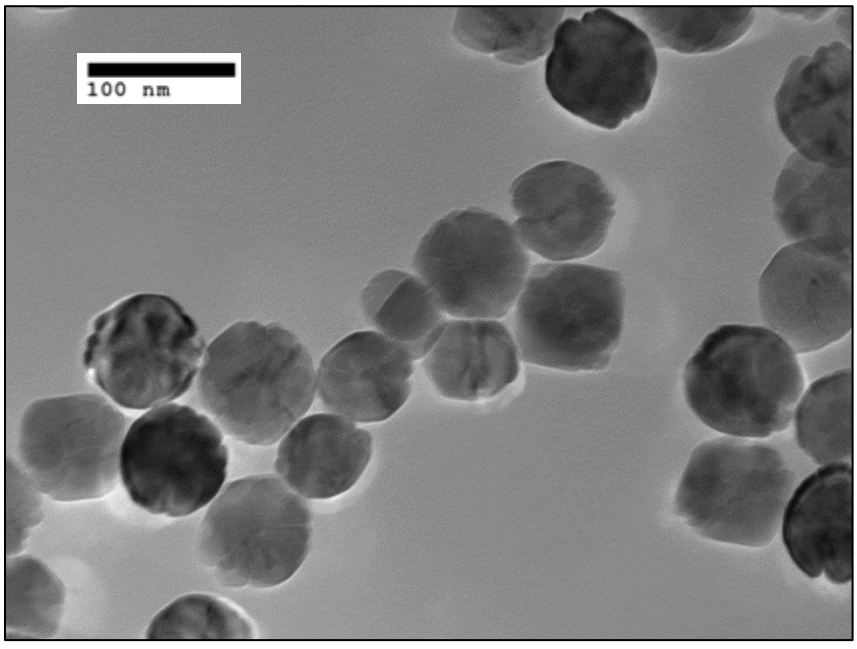

Figure 6: TEM image of hematite sample "Trial 1 8-29-12"

More images from the TEM analysis can be found in the Appendix. The TEM analysis exhibited the roughly spherical particles expected. Based on the scales shown in each image, the diameters were estimated and are shown in Table 2. The median diameter of the hematite nanoparticles was 75.75 ± 10.58 nm. Results were precise among trials but were not accurate relative to expected size. There are many factors in the hematite synthesis responsible for size control such as the acid concentration, aging time, and dissolution of ferric chloride in acid. With time as a constraint, the decision was made to forego the hematite samples or synthesis of new samples and use previously synthesized particles that were already determined to be 50 nm in size.

Table 2: Hematite size characterization based on TEM analysis

Hematite Size Characterization		
Trial 1 (8-29-12)	Median Diameter (nm)	75.63
	Standard Deviation	8.76
Trial 2 (9-10-12)	Median Diameter (nm)	75.87
	Standard Deviation	12.40
Average	**Median Diameter (nm)**	**75.75**
	Standard Deviation	**10.58**

The process for nanosilver synthesis was more delicate than that of hematite and several issues were encountered. Initial batches were not spherical particles and consisted of amorphous polygons. Subsequent attempts failed to turn into the characteristic vibrant orange color after the allotted reaction time had transpired. Two hypotheses were developed to explain this undesired outcome: light was breaching the solution and photolyzing the silver particles or the reagents, particularly ammonia, had degraded and were not at the required concentration. The light influence was tested first as the beaker was wrapped in aluminum foil and a cardboard box was placed over top of the beaker and stir plate. This did not have any apparent impact on the solution as it remained colorless after the allotted time. Once the reaction was prolonged a few

minutes longer, the solution had indeed turned a vibrant orange, however a longer reaction time typically yields larger particles with greater variability. Since ammonia is the primary contributor to particle size, a new stock solution was made and filtered prior to synthesis. A degrading ammonia solution proved to be the issue as the newly generated stock solution yielded the desired orange result after the expected reaction time. A TEM analysis further validated this theory as the particles were not only spherical, but accurate and precise with a median diameter of 48.45 ±8.43 nm. An image captured from the TEM analysis is shown in Figure 7 and more images can be found in the Appendix. Table 3 displays the estimated size characterization for two nanosilver samples synthesized.

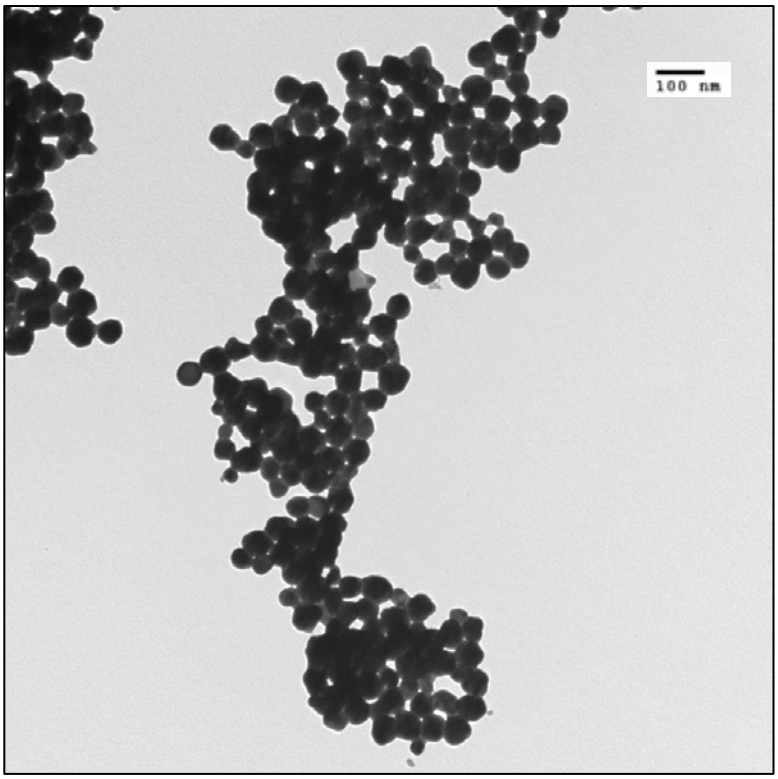

Figure 7: TEM image of nanosilver sample "Trial 1 2-27-13"

Table 3: Nanosilver size characterization based on TEM analysis

Nanosilver Size Characterization		
Trial 1 (2-27-13)	Median Diameter (nm)	50.91
	Standard Deviation	9.05
Trial 2 (2-27-13)	Median Diameter (nm)	45.99
	Standard Deviation	7.80
Average	**Median Diameter (nm)**	**48.45**
	Standard Deviation	**8.43**

3.2 Static Tests Involving Hematite

The static tests involving hematite were mainly initial experiments to become accustomed to the system before coupling to the flow-through cell. The benefit of the static system experiments was that they could be compared to a wealth of data previously collected by Noerpel et al [19]. Figure 8 shows spectra collected from citrate adsorbed to hematite wet paste solutions (HWP) compared to batch adsorption experiments (batch) from Noerpel et al [19] as a function of pH. The HWP samples were prepared by mixing a suspended hematite solution with citric acid at the designated pH. The mixed solution was then centrifuged and smeared onto the diamond IR crystal. In general, the HWP spectra appear similar to the batch spectra in the sense that all peaks are present at relatively the same wavenumber. The carbonyl stretch of the hematite wet paste at pH 3.74 (1700 cm^{-1}) was shifted to the right of the respective peak from the batch adsorption spectra (1715 cm^{-1}). Wavenumber shifts are not easily explained and this case may be due to poor subtracting or the influence of water adsorbed to the hematite surface. The difference in peak height corresponds to the batch solutions containing a much higher concentration of hematite than the HWP samples. The greatest issue with this procedure is the inability to accurately subtract the influence of hematite and water, evident from the difference in local minima surrounding the asymmetric stretch at 1570 cm^{-1}. These spectra were resolved by subtracting spectra from a HWP sample at similar citrate concentration by Noerpel et al [19].

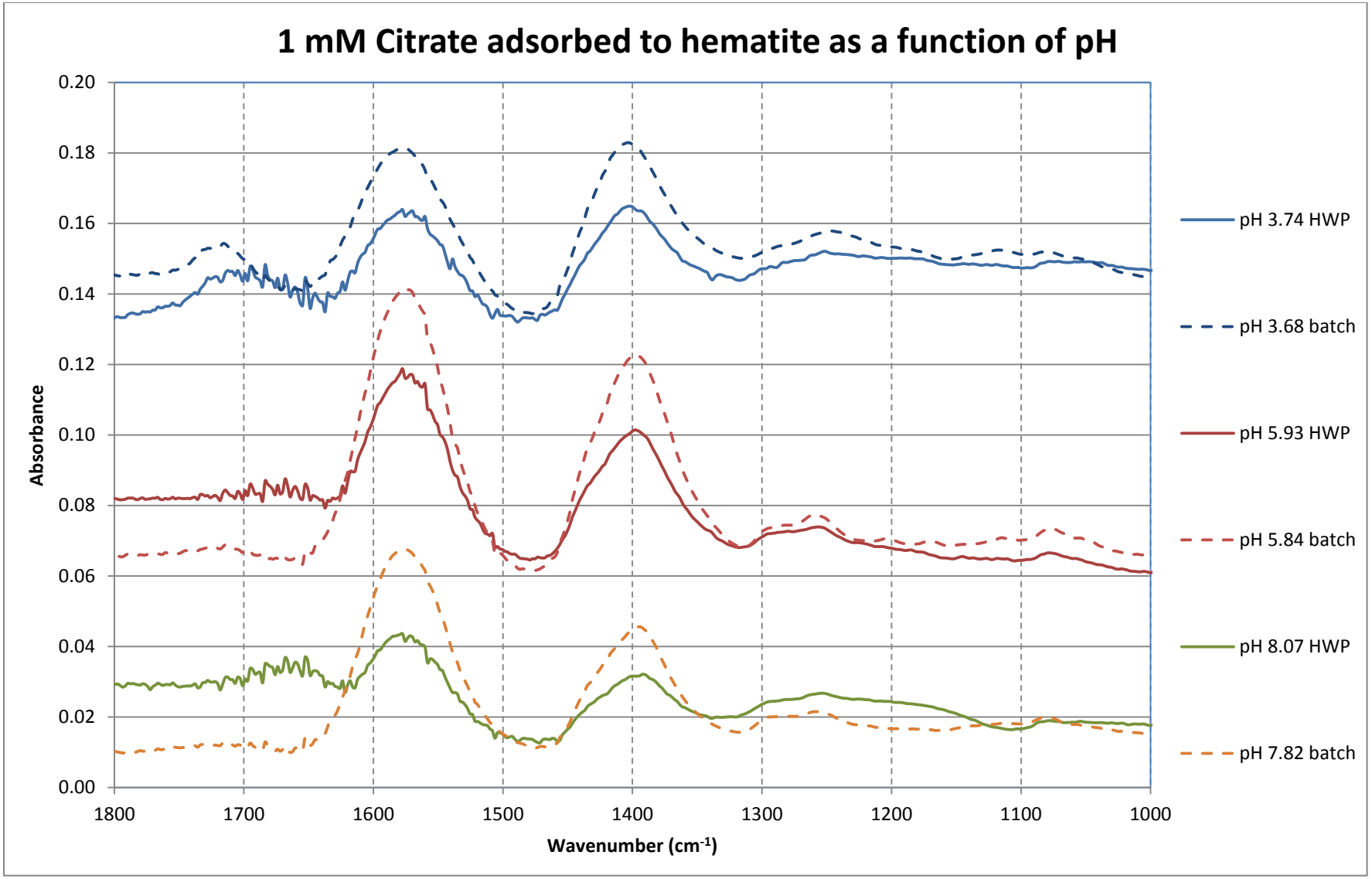

Figure 8: Citrate on hematite as a function of pH. Solid lines are the hematite wet paste (HWP) samples with a certain pH of citrate adsorbed to hematite. Dotted lines are hematite wet paste batch adsorptions (batch) from Noerpel et al [_]

It is clear from the difference in local minima and noise generated between 1600 cm^{-1} and 1800 cm^{-1} that subtracting arbitrary HWP spectra was not sufficient as each wet paste was unique.

One mM was chosen as the concentration for citrate because that was assumed to be an undetectable level in solution. The citrate that adsorbs to the hematite is present in much higher concentration and thus dominates the spectra. This assumption was validated by collecting spectra from 1 mM citrate in solution. The resulting spectrum was resolved by subtracting spectra obtained from deionized water. There was an evident peak around 1410 cm^{-1} that coincides with the location of the symmetric stretch; however, on a relative scale this peak did not influence that of citrate adsorbed to hematite. These results are displayed in Figure 9 and the citrate in solution spectra is multiplied by 10 to make the hydroxyl peak viewable.

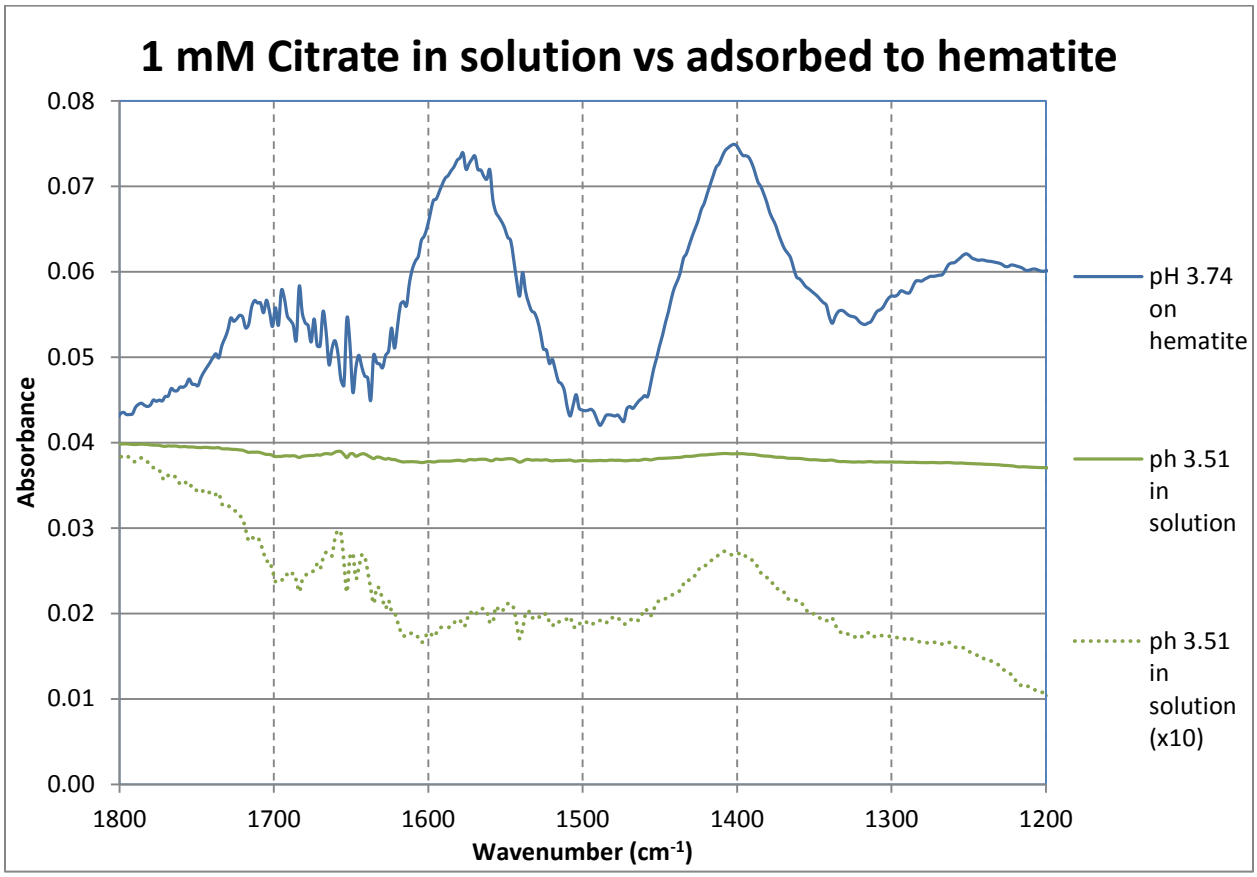

Figure 9: 1 mM citrate in solution (green) compared to 1 mM citrate adsorbed to hematite (blue)

Phthalic acid on hematite batch adsorption spectra from Lenhart et al. [20] was also used as a barometer to test the validity of the static system. Data was collected using an empty cell as the background, coating the diamond cell with hematite, and placing 0.1 mM phthalic acid on top. The resulting spectrum was resolved by subtracting out a previously collected deionized water spectra and an empty cell coated with hematite. These subtractions removed the influence of water from the diluted phthalic acid solution and hematite from the coated cell. Figure 10 is a juxtaposition of the resolved spectra and a batch adsorption experiment from Lenhart et al. [20].

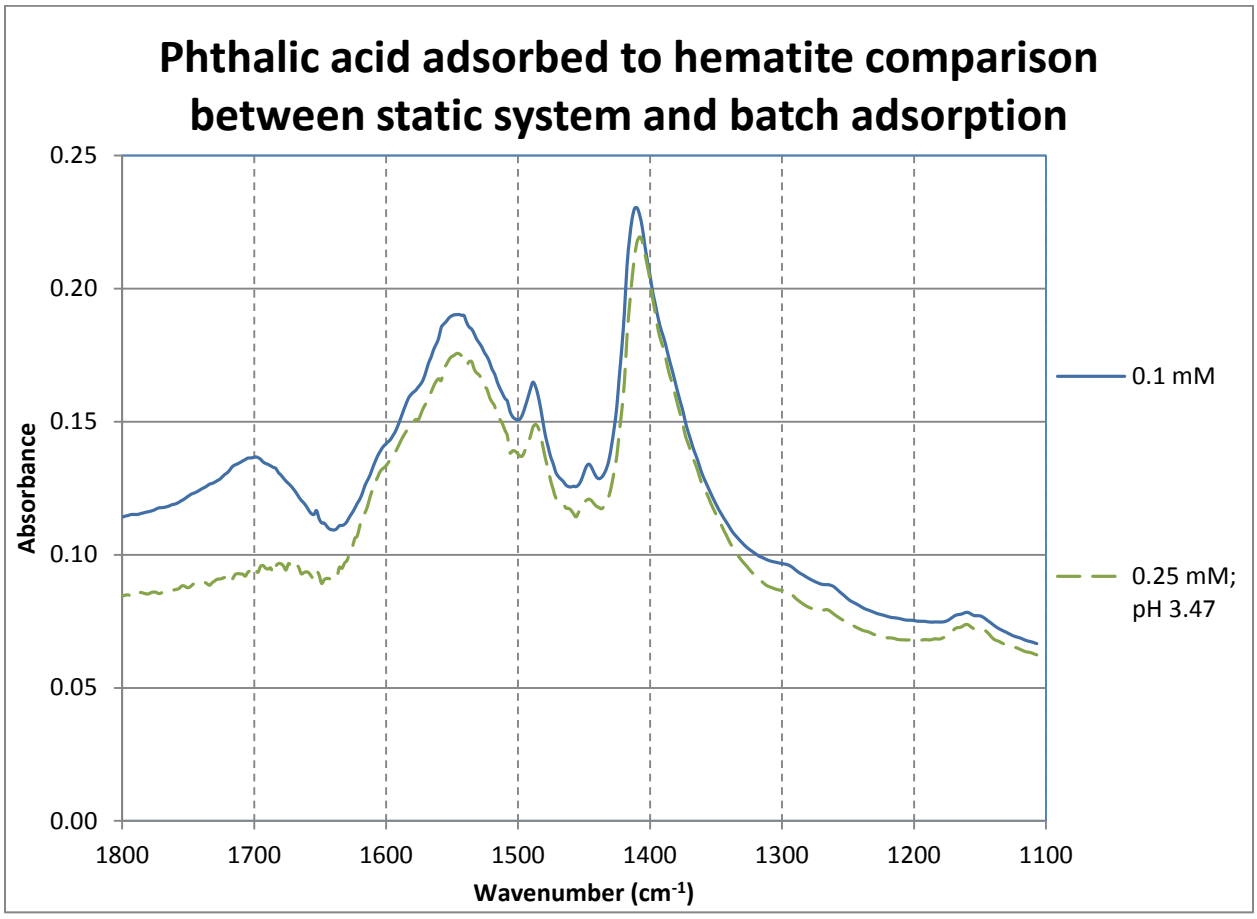

Figure 10: 0.1 mM phthalic acid solution adsorbed to hematite through the proposed static system compared to a batch adsorption from Lenhart et al. [20] using 0.25 mM phthalic acid at pH=3.47

The purpose of the comparison is to validate the static system and its ability to accurately detect the phthalic acid adsorbed to the hematite surface. In general, the two spectra appear similar to each other with two differences: the position of the symmetric stretch shifted slightly by 3 cm^{-1} and there is a relatively large peak in the static system spectra at 1700 cm^{-1} that is not evident in the batch adsorption spectra. The minor shift in the symmetric stretch can possibly be attributed to a difference in pH, although the pH of the static system test was not observed. The peak at 1700 cm^{-1} is likely an effect from the subtractions and potentially influenced by the water spectra. Neither difference is believed to dispute the validity of the static system.

3.3 Static Tests Involving Silver Nanoparticles

Unlike the hematite analyses, there was no existing data from nanosilver infrared analysis for comparison. In these regards, each reagent was analyzed at their respective concentrations from the synthesis process to ensure they were below a detectable limit and would not appear in the silver spectra. The spectra collected from 0.025 M D-maltose is displayed in Figure 11 along with spectra from deionized water and the subtraction of water from D-maltose in order to isolate the difference in spectra. The two curves are essentially identical until approximately 980 to 1180 cm^{-1} where the subtraction result has a peak at 1039 cm^{-1}. A similar test was performed for the 0.02 M ammonia solution; however, there was no discernible difference between the ammonia spectrum and that for water spectrum. These results indicated that a concentration of 0.02 M is lower than the detectable limit for ammonia in solution and therefore should not influence the silver spectra. Research shows that the nitrate ion has a significant peak around 1350 cm^{-1} [21].

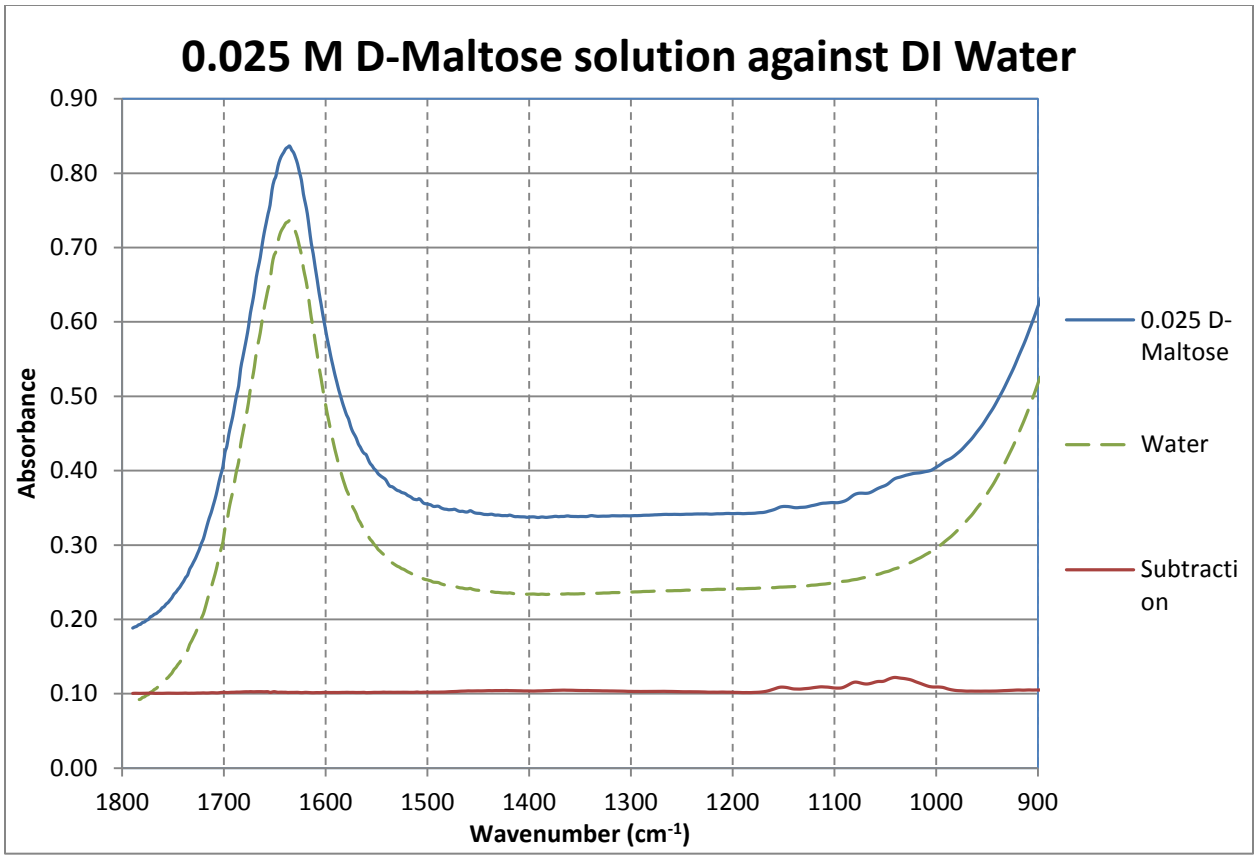

Figure 11: ATR-FTIR spectra of aqueous 0.025 M D-maltose solution against deionized water. The subtraction of deionized water from the diluted D-maltose solution is also shown so isolation of the difference in spectra.

Silver coating spectra were collected on the diamond cell using an empty cell as the background to determine if silver itself is IR active or if the reagents have a profound effect on the spectra. This step was not required for hematite because there was a great deal of previously collected data for comparison. Figure 12 depicts the influence of reagents on silver coating spectra. The silver coated cell exhibits three peaks: 1600 cm^{-1}, 1390 cm^{-1}, and 1090 cm^{-1}. The latter is the largest peak and coincides with the location of the D-maltose peak, albeit with a different shape. Also, the 1390 cm^{-1} peak could possibly be caused by the nitrate absorption of IR. Once water was placed on top of the silver coated crystal and the water spectrum was subtracted out, these two peaks became negative, signaling the removal of these substances. According to these results, any reagent left on the nanosilver is simply rinsed away when fluids are added and can

likely be removed with a longer dialysis period. There is also a newly developed peak around 1525 cm^{-1} once water is added. This can likely be attributed to water absorbing IR or poor resolution of the spectra.

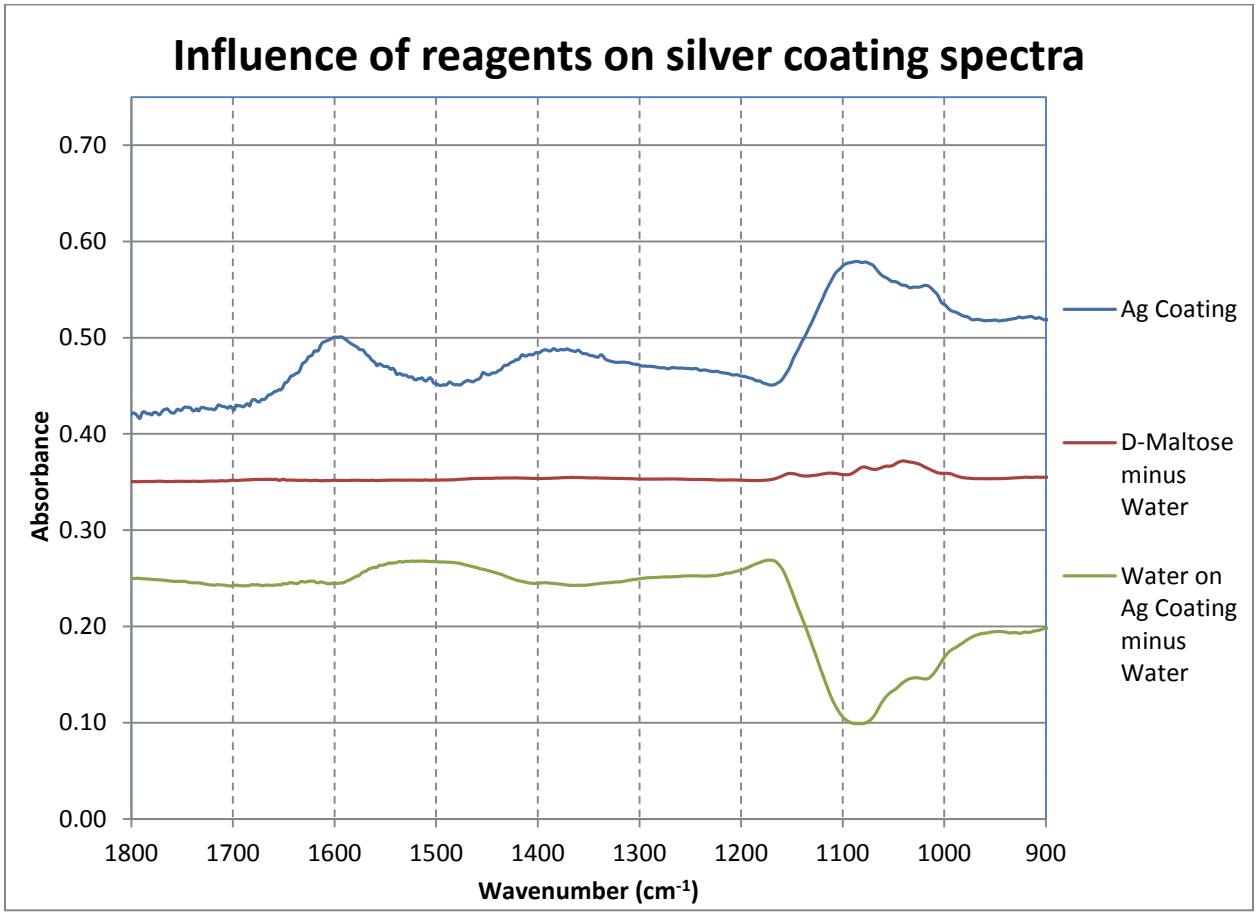

Figure 12: Influence of reagents from nanosilver synthesis on the spectra of the silver coated diamond cell. "Ag Coating" refers to the cell coated with a nanosilver suspension. "D-maltose minus Water" refers to the isolated D-maltose spectra without the influence of water. "Water on Ag Coating minus Water" refers to a cell coated with a nanosilver suspension and then filled with deionized water and the water spectra subtracted out.

Spectra obtained from citrate (1 mM) adsorbed to the surface of silver were compared to the citrate liquid phase spectra (200 mM) obtained by Noerpel et al [19]. These results are presented in Figure 13 as a function of pH. The relative peaks of citrate adsorbed to silver corresponded to those of the citrate solution at both pHs analyzed; however, at a pH of 4.9, the asymmetric peak around 1580 cm^{-1} and the symmetric peak around 1390 cm^{-1} of the citrate

adsorbed to silver greatly decreased relative to the liquid phase spectra. Since the carbonyl stretch (~1720 cm^{-1}) and the hydroxyl stretch (~1210 cm^{-1}) exhibited minimal change, the citrate is not changing structure in the sense it is not losing a proton or hydroxide. This leads credence to the belief that the citrate is adhering to the silver surface as an outer-sphere complex however, the loss of the asymmetric and symmetric peak signify an inner-sphere complex. In this case, no determination can be made as it is unexpected that the citrate is not changing structurally yet its movement is restricted. No attempt to replicate these results was attempted due to time constraints.

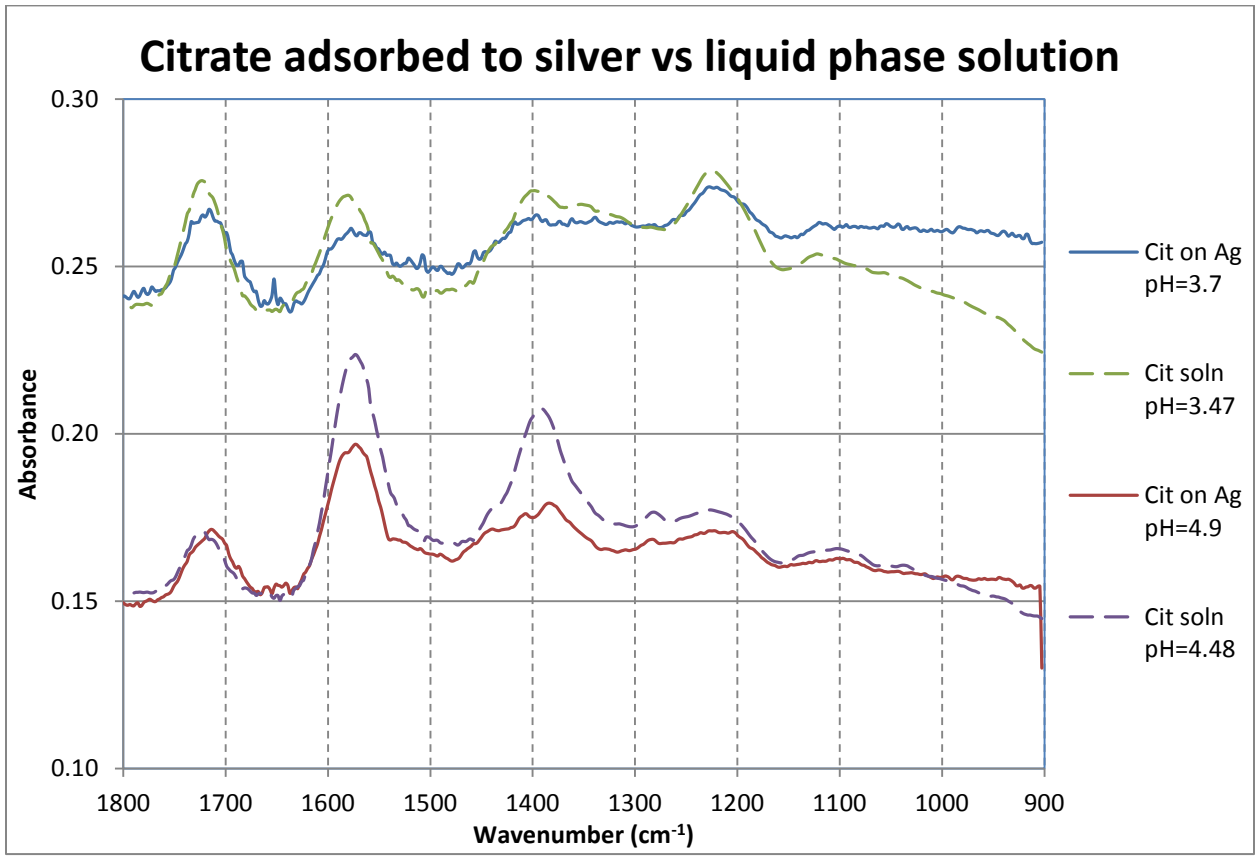

Figure 13: ATR-FTIR spectra comparing citrate (1 mM solution) adsorbed to the surface of nanosilver versus citrate (200 mM) in the liquid phase as a function of pH. The citrate adsorbed is shown in the solid lines while the citrate in solution appears as dotted lines.

3.4 Dynamic Tests Involving Hematite

The greatest difficulty involved with the tests utilizing the flow-through cell was removing the influence of water which has a significant presence in the location of interest. Another obstacle was allowing sufficient time for the citrate to adsorb or desorb as well as equilibrate before spectra could be collected. The dynamic test process evolved over time as different factors were manipulated. Figure 14 displays the evolution of the dynamic procedure in a graphical sense. The first test (1) with the flow-through cell involved passing a citrate solution (1 mM + 100 mM NaCl) over the coated cell starting at a low pH and titrating up with 0.1 M NaOH. In this procedure the samples were also open to the atmosphere. Initially, the cell was coated and background and empty cell spectra were subsequently collected. From there, the citrate adsorbed to hematite spectra were collected and those were resolved by subtracting spectra of the hematite coated cell with deionized water plus 100 mM NaCl at various pH values. There were several issues pertaining to this procedure: a heavy influence from the water adsorbed to hematite peak at 1640 cm^{-1}, an upwards drift in the pH between titrations, and the inability to accurately subtract noise using spectra obtained from a previously coated cell. The latter is due to the degree of difficulty involved with evenly coating the diamond cell across such a great area. The next experiment (2) dried the cell under a stream of nitrogen for an extended time upon coating, collected the hematite coated cell at various pH spectra prior to the citrate spectra, and started at a high pH before titrating down with 0.1 M HCl. Titrating down countered the pH drift and also potentially allowed the system to reach equilibrium sooner if the desorption process occurs faster than the sorption process as thought. The resulting spectra were resolved by subtracting the hematite coated cell at various pH spectra as well as an empty cell. Following subtractions, the spectra contained an even greater water influence and the pH drift

persisted. Tests (3) and (4) attempted to remove the water influence by collecting spectra relative to a background reading of the coated cell filled with deionized water. Also to control the pH drift, a steady nitrogen stream was bubbled through the sample and all samples were prepared with boiled deionized water. One possible explanation for the pH drift is that the carbonate in the atmosphere was dissolving in the solution and reacting with the hematite surface which can alter solution pH. Boiling the water and placing samples under nitrogen were initiated to remove the influence of carbonates in the atmosphere. The difference between (3) and (4) is the resolution process. Test (3) involved collecting spectra at various pH values of citrate solution and subsequently subtracting out an empty cell spectra collected prior to the introduction of citrate. This empty cell was simply the hematite coated cell filled with deionized water with the purpose of removing experimental noise. Test (4) involved subtracting out a previously collected water spectra followed by a dry empty cell to remove remaining noise. Neither method was successful as evident in Figure 14, due to the over-subtraction of the water peak. Test (5) was conducted in a similar manner as test (2) with the difference involving the subtraction. First, water was subtracted from two components: the hematite coated cell and citrate on hematite coated cell. The resulting spectra for the hematite coated cell were subsequently subtracted from the citrate on hematite coated cell spectra. Finally, an empty cell spectra was subtracted from the previous subtraction result to remove any remaining noise. Test (5) occasionally over-subtracted the water peak, yet resembles the expected spectra (6) the most.

Table 4: Summary of the various methodologies tested for the hematite coated flow-through cell. Methodology number corresponds to the spectra displayed in Figure 14

Methodology	Details of Methodology
(1)	Citrate solution at low pH titrated up. Water on coated cell collected afterwards
(2)	Cell dried for an extended time. Water on coated cell collected first followed by citrate solution at a high pH titrated down
(3)	Deionized water on coated cell as background using an empty cell to resolve
(4)	Deionized water on coated cell as background using a water spectrum to reslve
(5)	Samples collected similar as (2) but resolution was done by subtracting a water spectrum from all components
(6)	Batch adsorption experiment from Noerpel et al [19] used as a control

Figure 15 is the extrapolation of Test (5) over the gamut of pH values analyzed. The results at the higher pH values (5.48-8.75) exhibit the greatest "dip" due to the water over-subtraction. However, there is a clear carbonyl stretch (1720 cm^{-1}) in the pH = 3.51 spectra that decreases and extinguishes with increasing pH as expected. Also as pH increases, the skeletal stretch at 1300 cm^{1} becomes more refined which is also as expected.

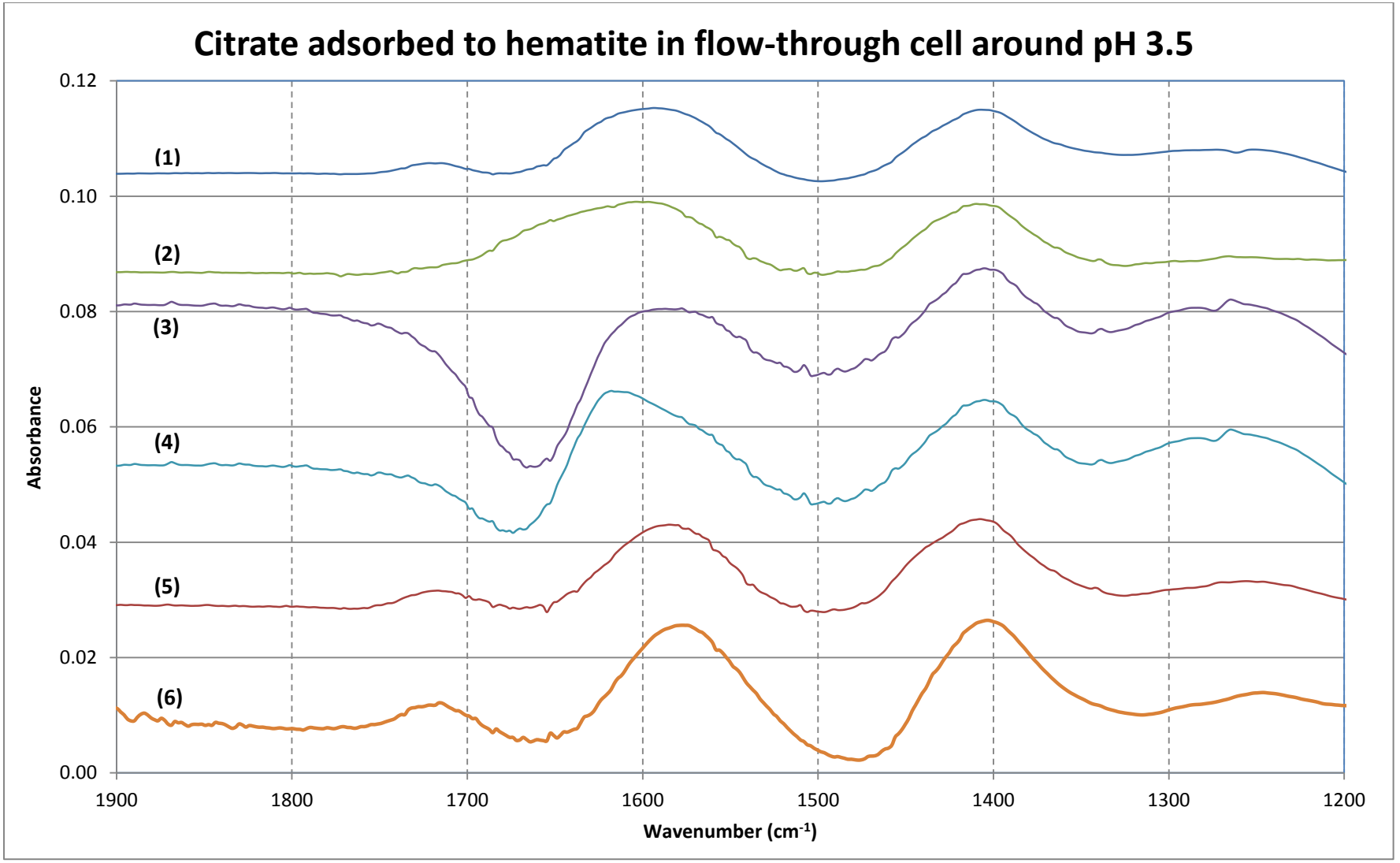

Figure 14: Citrate adsorbed to hematite in flow-through cell around pH 3.5. (1) is starting at a low pH and titrating up. (2) is starting at a high pH and titrating down. (3) is from using a deionized water-filled cell as a background. (4) is also from using a deionized water-filled cell as a background but subtracting out a water spectra. (5) is from an empty coated cell background and subtracting water from all components. (6) is the expected spectra that was obtained through batch adsorption experiments in Noerpel et al [19].

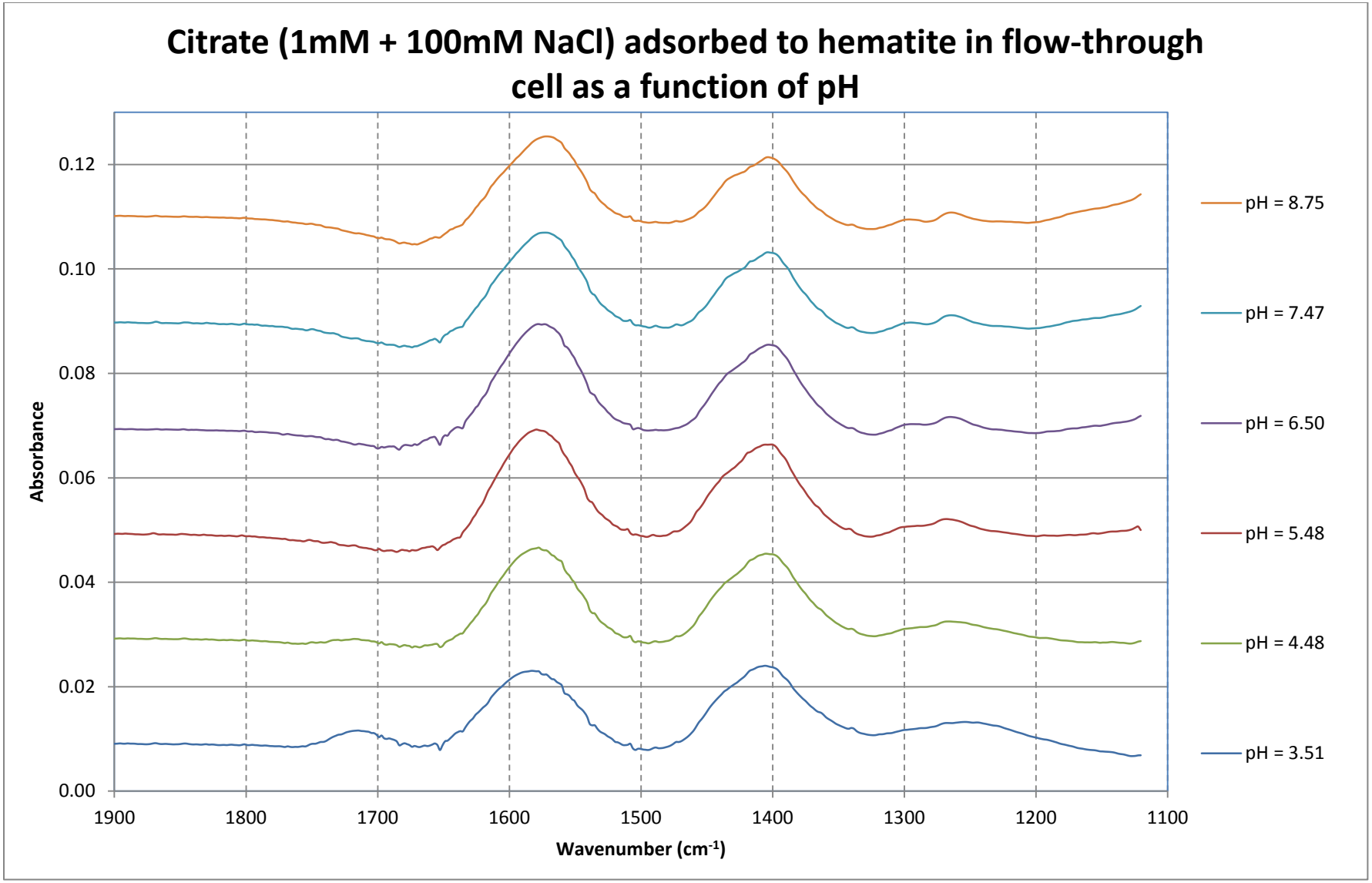

Figure 15: Spectra obtained from coating the flow-through cell with hematite and varying the pH of citrate

To analyze the validity of this method, a synchronous 2D correlation plot was developed comparing the movement of the spectra displayed in Figure 15 with an increase in pH. The intensity of a synchronous 2D correlation spectrum represents the simultaneous or coincidental changes of two separate spectral intensity variations over a defined variable [22]. As pH increased, simultaneous shifts between the data resulted in a positive peak (red) while opposing shifts resulted in a negative peak (dark blue). If no correlated movement occurred, the peak would remain at 0 (light blue/dark green).

The 2D correlation plot is displayed in Figure 16. The favorable results include the positive asymmetric peak (1570 cm^{-1}) and the subsequent positive peaks relating the asymmetric stretch to the symmetric stretch (1390, 1570). The asymmetric and symmetric stretches were expected to move simultaneously as pH increased. The carbonyl group (1720 cm^{-1}) is not prevalent in the correlation plot and the dark blue rings adjacent to the asymmetric peak signify a heavy water influence. The dark blue rings are known to correspond to the water because there should be no correlation or movement around 1640 cm^{-1} as there is no absorbance associated with citrate at that location. The influence of water can be observed in Figure 15 as the "dip" around 1640 cm^{-1} becomes more prevalent as pH is increased.

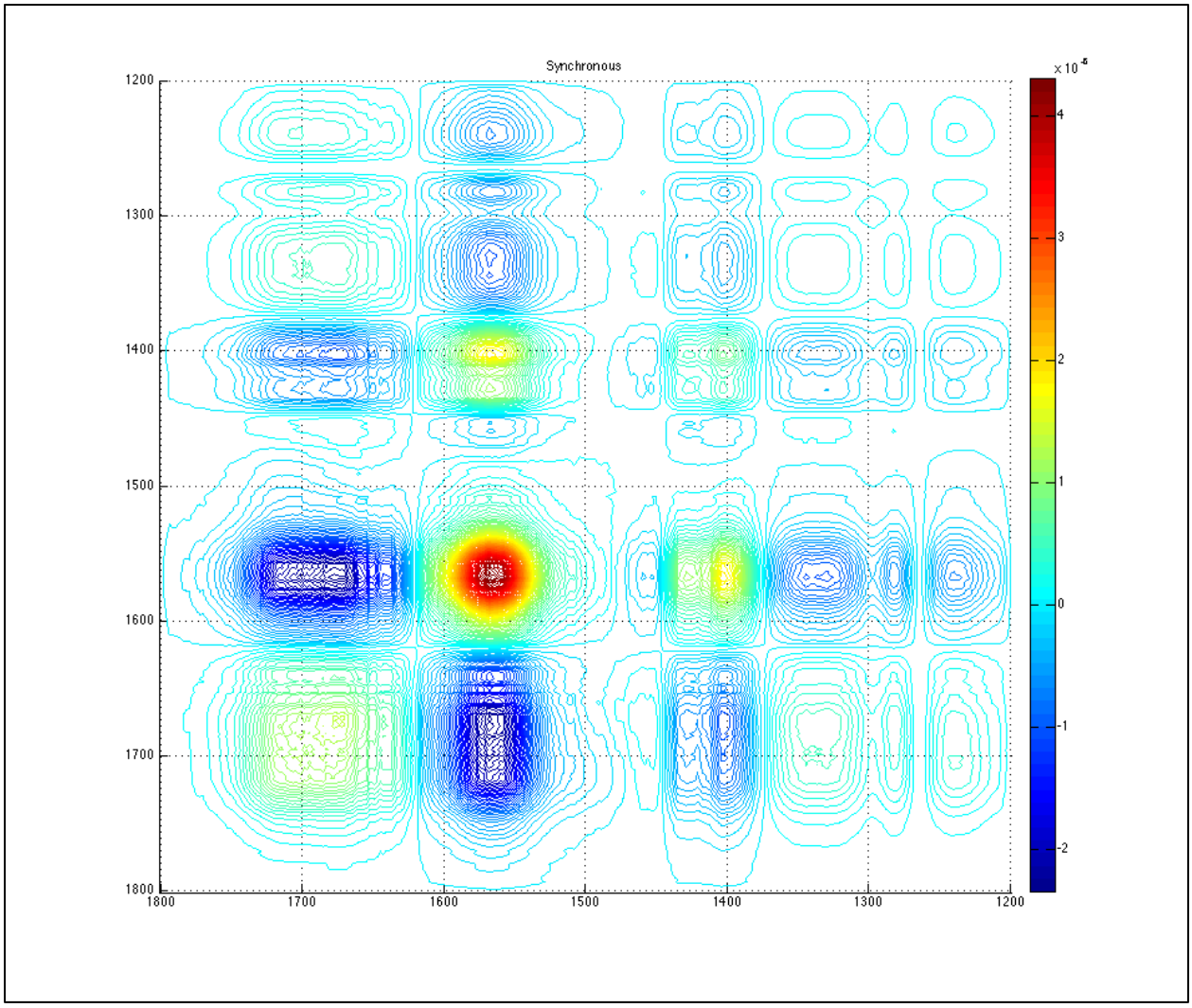

Figure 16: Synchronous 2D correlation plot comparing the spectra obtained from the flow-through cell experiments to the batch adsorption experiments by Noerpel et al.

3.5 Dynamic Tests Involving Silver Nanoparticles

Coating the flow-through cell with the suspended nanosilver solution did not achieve favorable results. Unlike the hematite experiments where the water influence was proving too significant, the silver did not appear to adhere to the crystal surface or adsorb citrate. Upon subtracting the water and empty cell spectra in the same manner as the hematite experiments, the result was ambiguous experimental noise. The silver coating on the diamond cell was

observable however on the diamond cell, the sample returned no peaks. It is possible that silver does not absorb infrared radiation in the location of interest and the diamond cell experiment was detecting the reagents from the synthesis process, i.e. nitrate and D-maltose, while the sample utilized in the flow-through cell was dialyzed to a greater degree to remove excess constituents. The spectra collected showed no appreciable difference between coating at various pH values and introducing citrate while varying pH. This result indicates that either no substance was adsorbing to the silver surface or the silver was no longer adhering to the crystal. Another possible explanation for the lack of detection is that the nanosilver solution is too diluted. Initially, 100 µL of 1:1 nanosilver to ethanol solution was used to coat the crystal. Additional experiments increased this mixture to 450 µL of nanosilver solution and 50 µL of ethanol. While a coating was evident upon termination of the experiment, the spectra collected resembled previous experiments with no appreciable difference between spectra.

The next step in developing the methodology should be to either test the original solution that appeared using the diamond cell to coat the flow-through cell or to test the most recent solution on the diamond cell. This test would determine if the nanosilver is experiencing difficulty adhering to the germanium crystal surface as opposed to the diamond cell.

Chapter 4:

Conclusions

The purposes for this study were to (1) develop a method to prepare a particle coated IR surface, (2) couple this to a flow-through cell for dynamic changes, and (3) implement the method for analysis. Initially, static tests were developed by coating the diamond cell and placing an aliquot of liquid on top. Results were favorable for hematite as both the citrate and phthalic acid coatings exhibited similar spectra to previous research. Results from the silver tests indicated that the citrate was readily adsorbing to the silver surface and was detectable. As pH was increased, the citrate adsorbed to silver experience no change in composition but the motion was restricted as the asymmetric and symmetric stretches significantly decreased. No attempt was made to replicate these results due to time constraints. The static test was considered a success for both the hematite and silver materials however; accommodations should be made in the future to reduce the influence of water in the spectra.

The dynamic system was created by coupling the static system to a flow-through cell and allowed for increased control over variability. The dynamic system also presented many challenges, namely removing the influence of water in the spectra. The optimal method was to subtract a deionized water spectrum from all components before resolving the spectra. A synchronous 2D correlation plot compared the movement of the spectra as pH was increased and revealed that this method did not completely remove the influence of water and failed to accurately detect the carbonyl group. Tests involving the nanosilver solution were unsuccessful as the silver was not readily adhering to the crystal surface.

The methodology discussed in this study may not be perfected, but the foundation has been laid for future research to expand upon. Significant progress has been made and once the

influence of water is controlled, these processes should be capable of analyzing a multitude of nanomaterials and capping agents.

Appendix

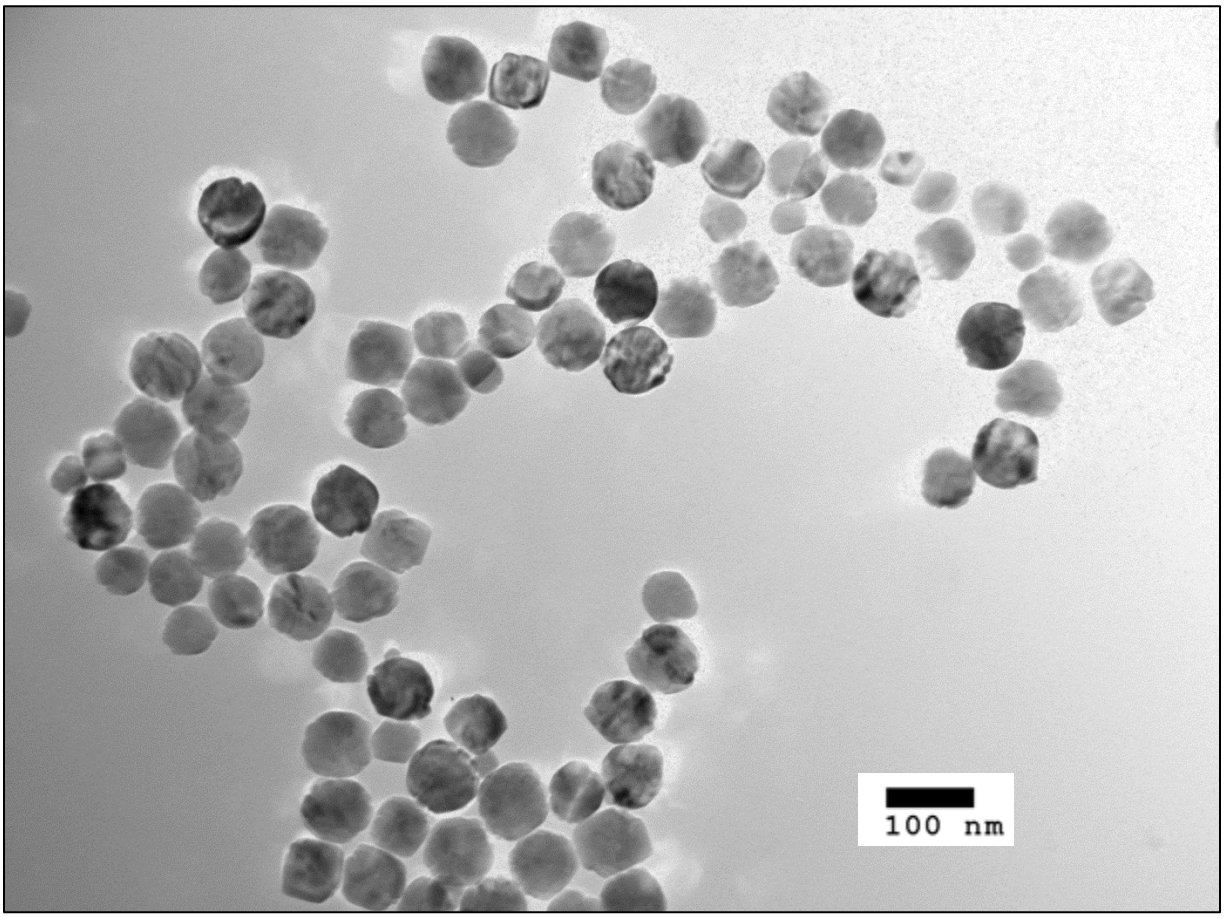

1: TEM image of synthesized hematite from 8/29/12

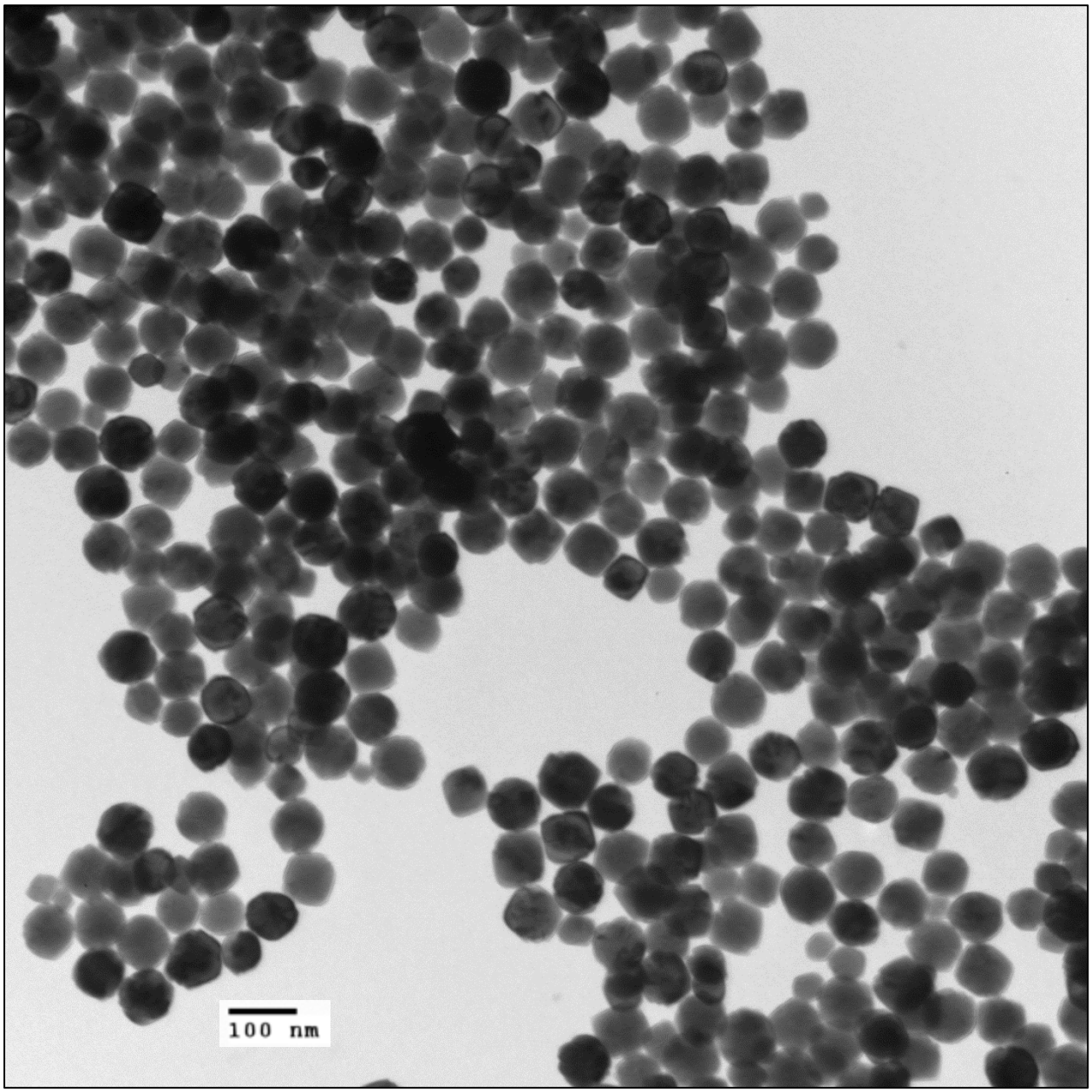

2: TEM image of synthesized hematite from 9/10/12

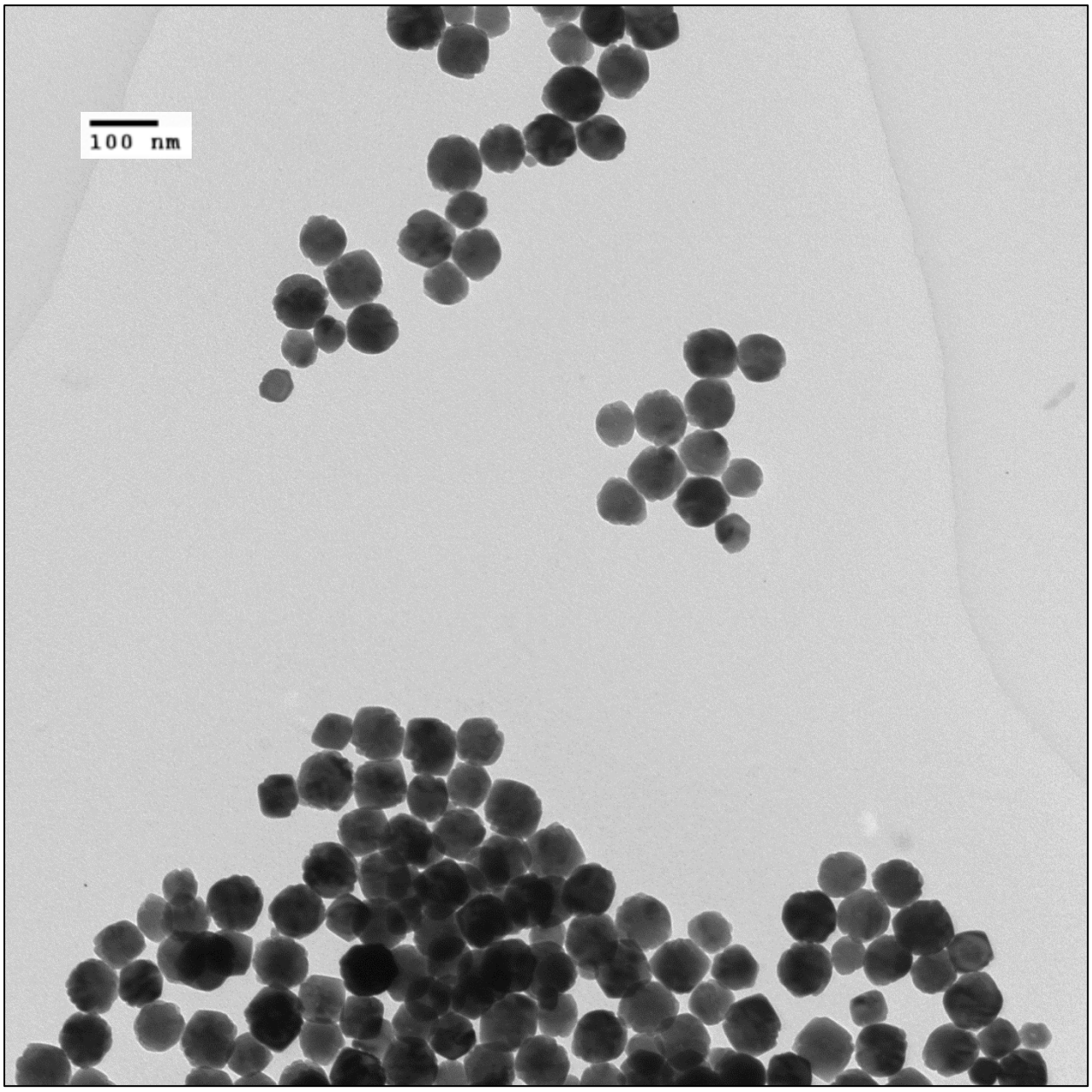

3: TEM image of synthesized hematite from 9/10/12

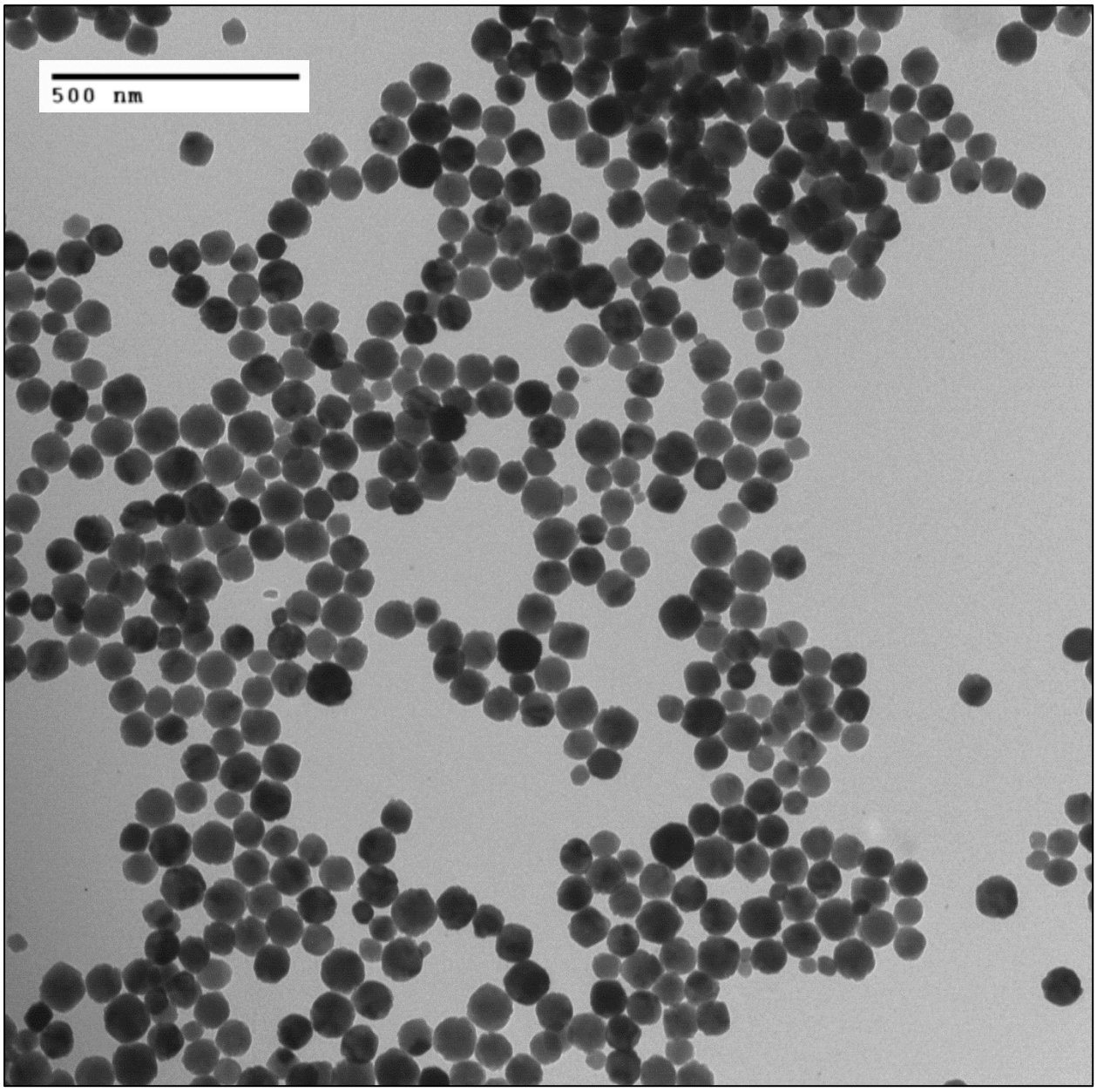

4: TEM image of synthesized hematite from 9/10/12

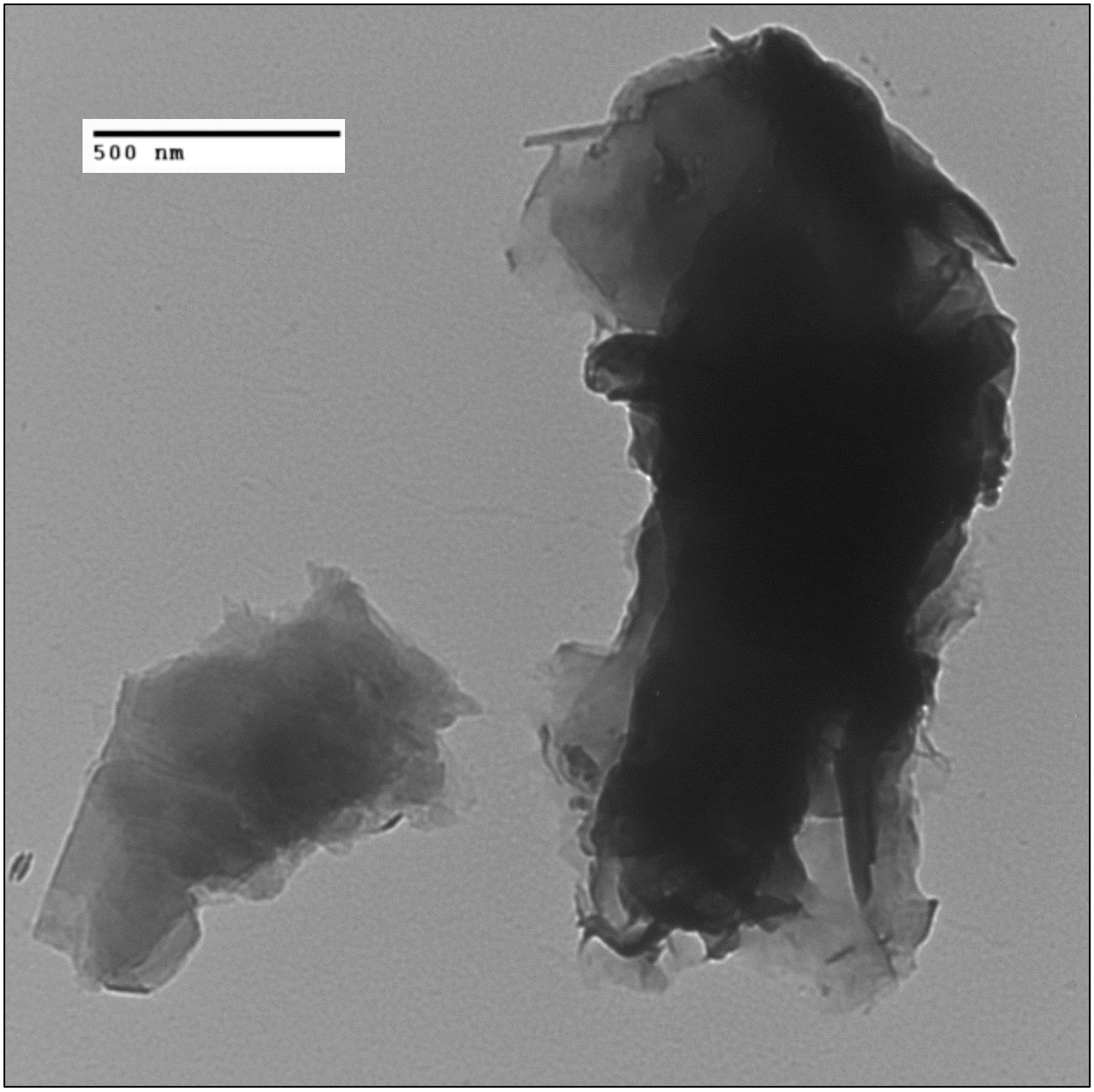

5: TEM image of first batch of synthesized nanosilver from 12/13/12

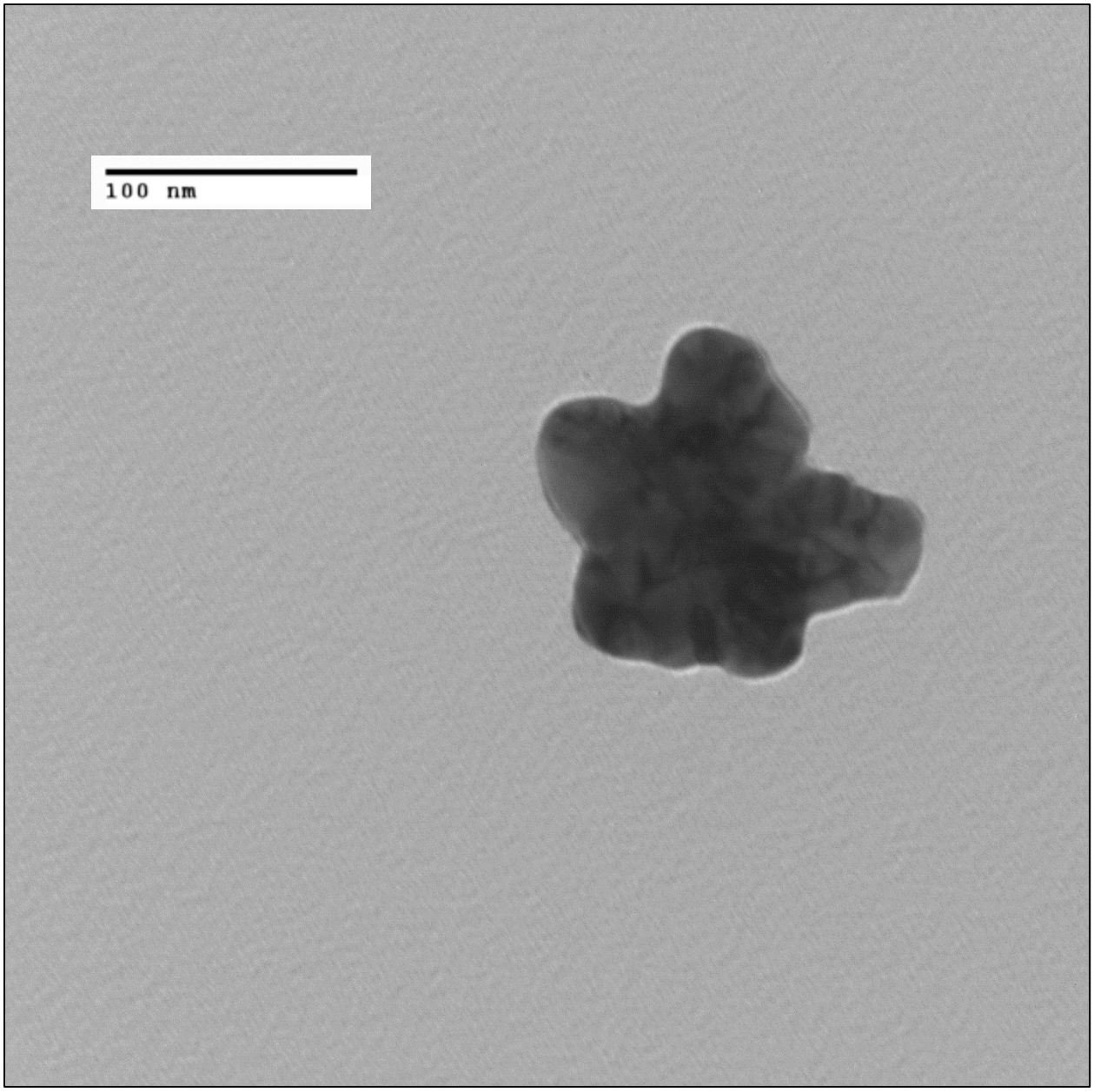

6: TEM image of first batch of synthesized nanosilver from 12/13/12

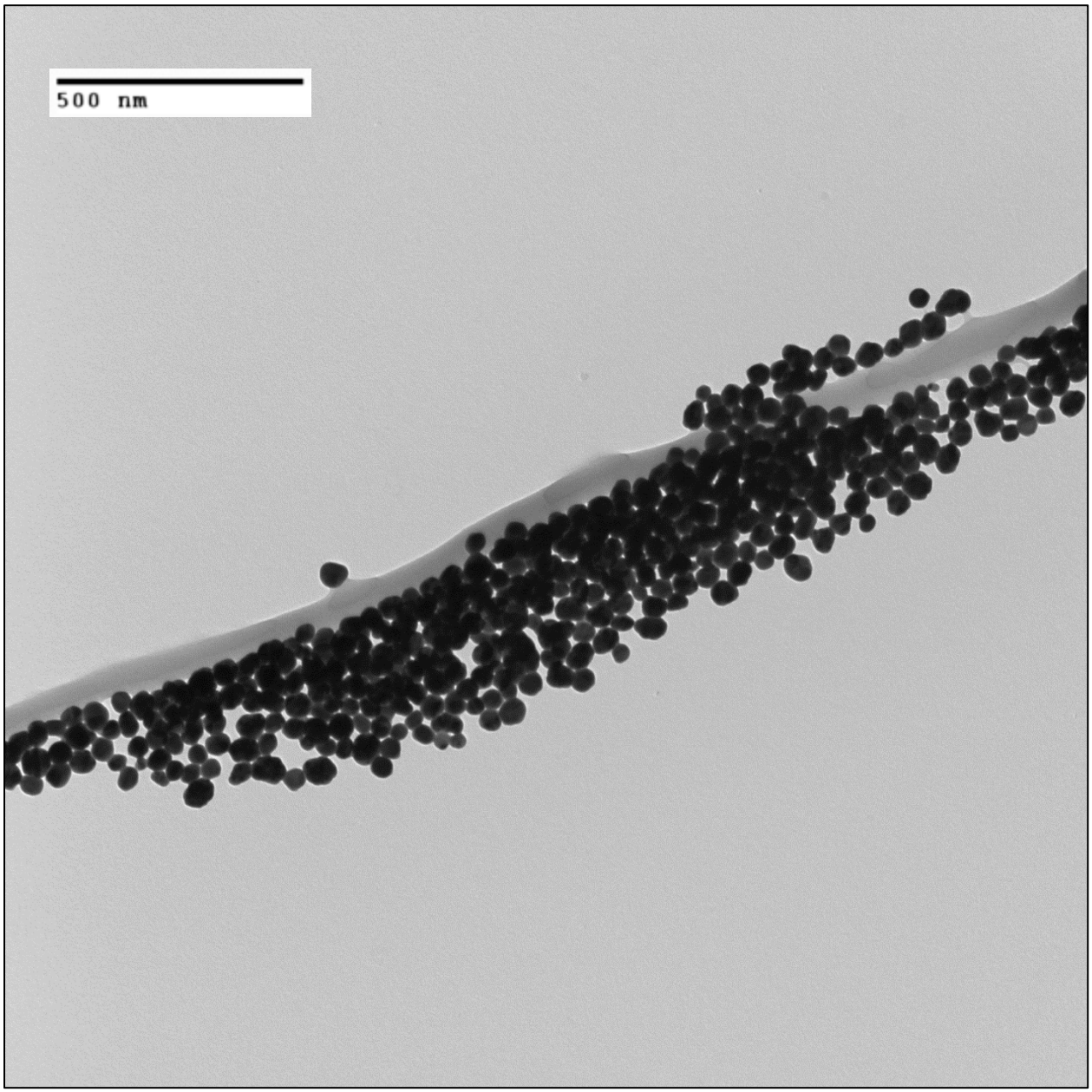

7: TEM image of second batch of synthesized nanosilver from 2/27/13

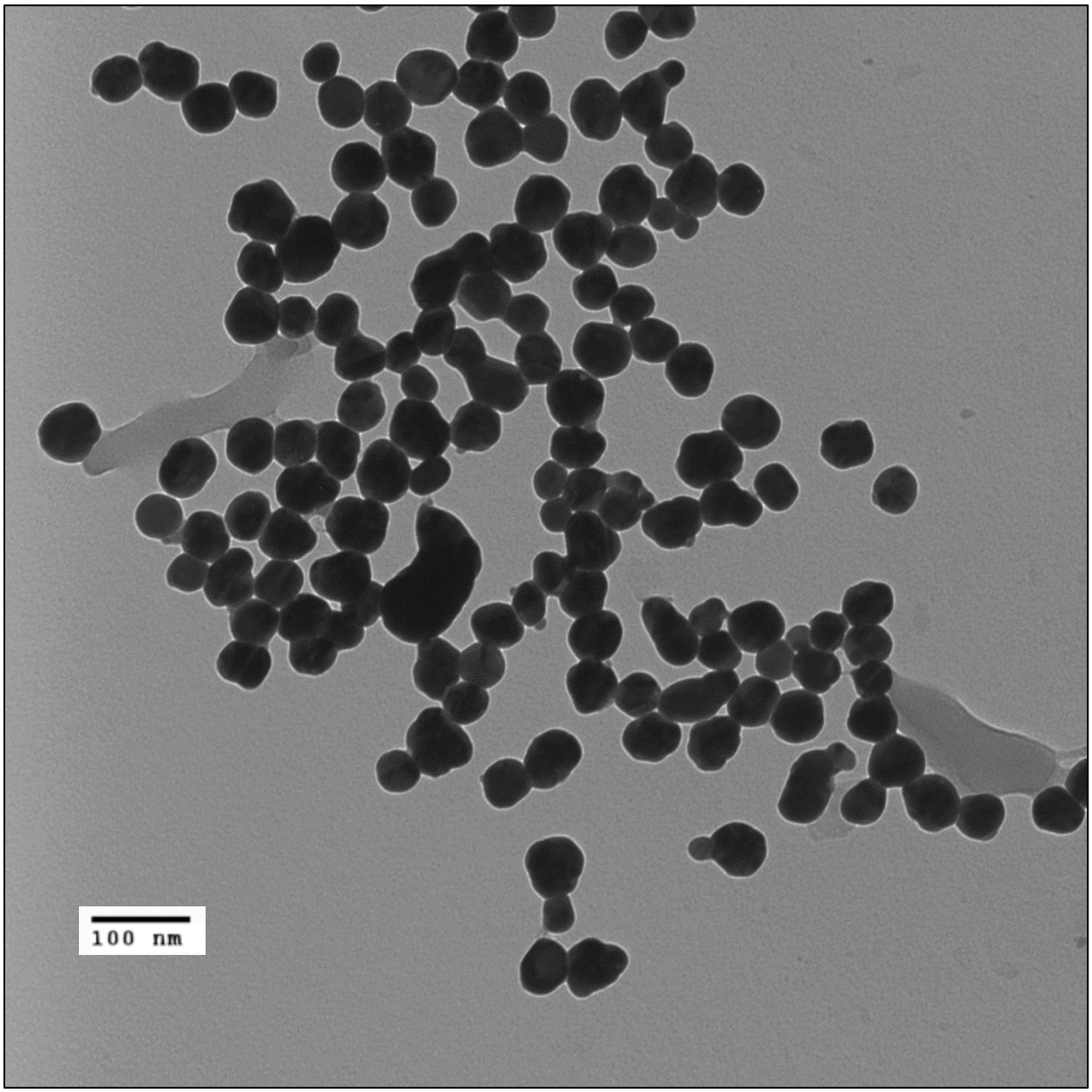

8: TEM image of second batch of synthesized nanosilver from 2/27/13

References

[1] Rotello, V.M., *Nanoparticles : building blocks for nanotechnology*. 2004, New York: Kluwer Academic/Plenum Publishers. p. 284

[2] Roco M, Brainbridge WS. *Societal Implications of Nanoscience and Nanotechnology*. 2001, Kluwer Academic Pubishers

[3] Niemeyer, C.M., *Nanoparticles, proteins, and nucleic acids: Biotechnology meets materials science.* Angewandte Chemie-International Edition, 2001. **40**(22): p. 4128-4158.

[4] Poole, C.P. and F.J. Owens, *Introduction to nanotechnology*. 2003, Hoboken, NJ: J. Wiley. xii, p. 388

[5] Schmid, G., *Nanoparticles : from theory to application*. 2nd ed. 2010, Weinheim: Wiley-VCH. xiii, 522 p.

[6] Kumar C. *Nanomaterials-Toxicity, Health and Environmental Issues*. Weinheim, Germany: Wiley-VCH; 2006.

[7] Benn, T.M. and P. Westerhoff, *Nanoparticle silver released into water from commercially available sock fabrics*. Environmental Science & Technology, 2008. 42(11): p. 4133-4139.

[8] Wang XJ, Ruedas-Rama MJ, Hall EAH. *The emerging use of quantum dots in analysis*. Analytical Letters 2007;40:1497–520.

[9] Wiesner, M.R. *Responsible development of nanotechnologies for water and wastewater treatment*. in *3rd IWA Leading-Edge Conference Water and Wastewater Treatment Technologies*. 2005. Sapporo, Japan.

[10] Wiesner, Mark R., Greg V. Lowry, Pedro Alvarez, Dianysios Dionysiou, and Pratim Biswas. *Assessing the Risks of Manufactured Nanomaterials*. Environmental Science and Technology, 2006, 40(14): p. 4336-4345.

[11] Li, Xuan. *Fate of Silver Nanoparticles in Surface Water Environments*. Diss. The Ohio State University, 2011.

[12] Hussain, S., et al., *In vitro toxicity of nanoparticles in BRL 3A rat liver cells.* Toxicology in Vitro, 2005. **19**(7): p. 975-983.

[13] Hanson, Natalie, Jeffrey Harris, Lauretta Joseph, Kalpana Ramakrishnan, and Thane Thompson. *EPA Needs to Manage Nanomaterial Risks More Effectively*. Report No. 12-P-0162. U.S. Environmental Protection Agency, 29 Dec. 2011. Web.

[14] Lead, Jamie R., Ju-Nam, Yon. *Manufactured nanoparticles: An overview of their chemistry, interactions and potential environmental implications.* Science of the Total Environment, 2008, 400(1-3): p. 396-414

[15] E. Matijevic, P. Scheiner, *Ferric hydrous oxide sols 1 2: III. Preparation of uniform particles by hydrolysis of Fe(III)-chloride, -nitrate, and -perchlorate solutions*. Journal of Colloid and Interface Science, 1978, 63(3): p. 509-524

[16] Kvitek, L. et al., *The influence of complexing agent concentration on particle size in the process of SERS active silver colloid synthesis*. Journal of Materials Chemistry, 2005, 15: p. 1099-1105.

[17] Borer, P. et al., *Photolysis of Citrate on the Surface of Lepidocrocite: An in situ Attenuated Total Reflection Infrared Spectroscopy Study*. The Journal of Physical Chemistry, 2007, 111(28): p. 10560–10569.

[18] Panacek, Ales., et al. (2006). "Silver Colloid Nanoparticles: Synthesis, Characterization, and their Antibacterial Activity." J. Phys. Chem. B 110(33): 16248-16253.

[19] Noerpel et al 2010, *research in progress*

[20] Hwang, Yu Sik, Liu, Jin, Lenhart, John J., Hadad, Christopher M., *Surface complexes of phthalic acid at the hematite/water interface*. Journal of Colloid and Interface Science, 2007. 307(1): p. 124-134.

[21] National Institute of Standards and Technology (NIST), Standard Reference Data, <http://webbook.nist.gov/chemistry/name-ser.html> Accessed on: 3/20/2013

[22] Noda and Ozaki, *Two-Dimensional Correlation Spectroscopy*. *Applications in Vibrational and Optical Spectroscopy*. John Wiley & Sons, Ltd. 2004